

JGR Atmospheres

-

RESEARCH ARTICLE

10.1029/2025JD044452

Key Points:

- Ice nucleating particles, cloud droplet number and phase partitioning parametrizations are crucial for correctly simulating mixed-phase clouds
- All these processes impact the radiation budget of the Southern Ocean, generally with common responses, but biases that vary case to case
- The default Unified Model parametrization overestimates cloud droplets numbers and ice nucleating particles over the Southern Ocean

Supporting Information:

Supporting Information may be found in the online version of this article.

Correspondence to:

D. K. E. Smith, d.smith5@uea.ac.uk

Citation:

Smith, D. K. E., Renfrew, I. A., van den Heuvel, F., Lachlan-Cope, T., Crawford, I., Bower, K., et al. (2025). The impact of mixed-phase cloud processes on simulating Southern Ocean clouds and their radiative effect. *Journal of Geophysical Research: Atmospheres, 130*, e2025JD044452. https://doi.org/10.1029/2025JD044452

Received 17 JUN 2025 Accepted 28 OCT 2025

Author Contributions:

Conceptualization: Daniel K. E. Smith, Ian A. Renfrew, Tom Lachlan-Cope, Paul Field

Data curation: Daniel K. E. Smith, Floortje van den Heuvel, Tom Lachlan-Cope, Michael Flynn

Formal analysis: Daniel K. E. Smith, Floortje van den Heuvel, Tom Lachlan-Cope, Ian Crawford, Keith Bower

© 2025. Crown copyright and The Author(s). This article is published with the permission of the Controller of HMSO and the King's Printer for Scotland. This is an open access article under the terms of the Creative Commons Attribution License, which permits use, distribution and reproduction in any medium, provided the original work is properly cited.

The Impact of Mixed-Phase Cloud Processes on Simulating Southern Ocean Clouds and Their Radiative Effect

Daniel K. E. Smith¹, Ian A. Renfrew¹, Floortje van den Heuvel², Tom Lachlan-Cope², Ian Crawford³, Keith Bower³, Michael Flynn³, Matthew D. Evans⁴, Steven J. Abel^{4,5}, and Paul Field^{4,5}

¹School of Environmental Sciences, University of East Anglia, Norwich, UK, ²British Antarctic Survey, Cambridge, UK,

Abstract Over the Southern Ocean, atmospheric and climate models have large biases in their radiative fluxes, primarily caused by the representation of supercooled liquid and mixed-phase low-level clouds, both at the macro- and micro-scale. The radiation biases lead to errors in simulated sea surface temperature, sea ice properties and large-scale atmospheric circulation. We assess the performance of a convection-permitting configuration of the Met Office Unified Model in simulating cloud over the Southern Ocean. We utilize aircraft and satellite observations from several cases in February 2023 during the Southern Ocean Clouds field experiment. We investigate the representation of three mixed-phase characteristics, namely ice nucleating particles (INP), the droplet number concentration and the spatial distribution of liquid and ice in mixed-phase clouds. A lower temperature-dependent INP concentration (based on synchronous INP measurements) results in lower ice mass and number concentrations that are closer to observations, and a higher cloud liquid water content. This reduces the net surface cloud radiative effect by up to 14 W m⁻². Reducing the droplet number to the campaign average had a similar sized impact on the cloud radiative effect (up to 22 W m⁻²) but opposite in sign, highlighting these compensating errors. Similarly, changing how well mixed the clouds are leads to a large sensitivity in the cloud radiative effect (up to 31 W m⁻²). All three mixed-phase processes play a crucial role in correctly modeling mixed-phase clouds and their impact on the radiation budget over the Southern Ocean.

Plain Language Summary Clouds over the Southern Ocean play a crucial role in the global climate system and low-lying clouds are challenging to simulate correctly in weather and climate models. Low-lying clouds over the Southern Ocean often contain a mixture of liquid water droplets and ice crystals, which interact in various ways. We investigate the representation of liquid droplets and ice crystals, and their interactions, in models. We compare our model simulations to measurements of clouds taken by aircraft- and satellite-borne instruments. We explore how improving the representation of these key processes impacts the amount of radiation that reaches the surface, highlighting that correctly modeling these processes is crucial for improving simulations of clouds over the Southern Ocean.

1. Introduction

Clouds over the Southern Ocean (SO) play an important role in regulating the climate. Representing these clouds in atmospheric and climate models is crucial for accurately simulating both the current climate and understanding their influence in a warming climate. However, most of these models have biases in their short and long wave radiation fluxes over the SO (Bodas-Salcedo et al., 2014; Cesana et al., 2022; Hyder et al., 2018), leading to significant errors in their sea surface temperature (Lauer et al., 2018). The primary cause for these biases is the representation of supercooled liquid/mixed-phase low-level clouds, both at the macro- and micro-scale (Bodas-Salcedo et al., 2019; Fiddes et al., 2022; Hyder et al., 2018). Recent model improvements have resulted in a reduction in these radiation flux errors, but significant biases remain (Gettelman et al., 2020; Lauer et al., 2022). In this study, we examine the representation of low-level clouds in several cases using new aircraft and ground-based in situ and satellite observations over the Bellinghausen Sea, in the SO.

Uncertainties in the processes that occur in mixed-phase clouds are one of the main causes of inaccurate radiative properties of clouds, particularly over the SO where the aerosol concentrations and properties are unique and poorly known (e.g., Atlas et al., 2020, 2022; Vergara-Temprado et al., 2018; Vignon et al., 2021). Primary ice production in atmospheric models is often designed to model ice nucleating particle (INP) properties in the

SMITH ET AL. 1 of 22

³Department of Earth and Environmental Science, University of Manchester, Manchester, UK, ⁴Met Office, Exeter, UK, ⁵School of Earth and Environment, University of Leeds, Leeds, UK



Journal of Geophysical Research: Atmospheres

10.1029/2025JD044452

Tom Lachlan-Cope
Methodology: Daniel K. E. Smith, Ian
A. Renfrew, Floortje van den Heuvel,
Tom Lachlan-Cope, Ian Crawford,
Paul Field
Project administration: Ian A. Renfrew,
Tom Lachlan-Cope
Visualization: Daniel K. E. Smith
Writing – original draft: Daniel
K. E. Smith, Ian A. Renfrew
Writing – review & editing: Daniel
K. E. Smith, Ian A. Renfrew, Floortje van
den Heuvel, Tom Lachlan-Cope,
Ian Crawford, Keith Bower, Matthew
D. Evans, Steven J. Abel, Paul Field

Funding acquisition: Ian A. Renfrew,

Northern Hemisphere (e.g., Cooper, 1987). However, observations show that the INP concentrations are significantly lower in the SO and Antarctic (McCluskey et al., 2018; McFarquhar et al., 2021; Uetake et al., 2020; Vignon et al., 2021). Over prescribing the concentrations of INPs in models can lead to the erroneous glaciation of clouds reducing their shortwave cooling effect (Sauerland et al., 2024; Vergara-Temprado et al., 2018; Vignon et al., 2021). Here, we use INP measurements from Rothera Research Station to constrain our simulations.

Additionally, liquid droplet number concentrations within mixed-phase clouds are often poorly represented in models over the SO (McCoy et al., 2020; Revell et al., 2019; Zhou et al., 2021). Lower cloud condensation nuclei (CCN) concentrations result in lower droplet numbers reducing the albedo of clouds via the Twomey effect (the first indirect effect) and the second indirect effects (e.g., Pincus & Baker, 1994). Thus, inaccurate representation of cloud droplet number concentrations can lead to biases in the short and long wave radiation fluxes in models (Gettelman et al., 2020; Zhou et al., 2021). Here, we use our aircraft observations to examine model sensitivity to cloud droplet number.

The liquid and ice phases within mixed-phase clouds can be mixed or partitioned on a variety of length scales (Field et al., 2004; D'Alessandro et al., 2021; Korolev & Milbrandt, 2022). Cloud droplets and ice particles can be uniformly distributed (genuinely mixed) or spatially separated (conditionally mixed). In genuinely mixed clouds, the growth of ice particles and evaporation of liquid droplets, by the Wegener-Bergeron-Findesen (WBF) process (Bergeron et al., 1935; Findeisen, 1938; Wegener et al., 1911) and riming, eventually leads to the glaciation of mixed-phase clouds. The spatial distribution of ice and liquid water at scales appropriate to model resolutions is, however, poorly constrained by observations and consequently, how this is represented in models can either enhance or limit the rate at which they become glaciated (Abel et al., 2017; Tan & Storelvmo, 2016), potentially modifying the radiative fluxes. We also examine model sensitivity to phase partitioning in mixed-phase clouds.

One challenge for addressing the biases over the SO is the lack of in situ cloud microphysical observations. Recent campaigns have obtained valuable in situ observations (e.g., Lachlan-Cope et al., 2016; McFarquhar et al., 2021; O'Shea et al., 2017) which have led to model evaluation studies (e.g., Atlas et al., 2020; Atlas et al., 2022; Gettelman et al., 2020; Järvinen et al., 2022; Listowski & Lachlan-Cope, 2017; Young et al., 2019). However, this is still a relatively small number of studies compared to other regions. Ice number concentrations in the Polar Weather Research and Forecast (WRF) model have been assessed focusing on primary (Listowski & Lachlan-Cope, 2017) and secondary ice production (Young et al., 2019) over the Antarctic Peninsula and Weddell Sea respectively. There have been detailed model comparisons with the Southern Ocean Clouds, Radiation, Aerosol Transport Experimental Study (SOCRATES) aircraft observations (McFarquhar et al., 2021). For example, Atlas et al. (2022) compared the global version of the System for Atmospheric Modeling (gSAM, Stevens et al., 2019) with five different microphysics schemes showing that those with an adequate representation of the Hallet-Mossop process (Hallett & Mossop, 1974) have a reduced bias in shortwave radiative fluxes compared to satellite observations and better particle size distributions compared to in situ measurements. Gettelman et al. (2020) used the Community Atmosphere Model 5 (CAM5) and CAM6 and the SOCRATES observations to highlight process level understanding of model biases and demonstrate the benefits of a two-moment microphysics scheme that is able to produce more supercooled liquid water—closer to that observed.

Here, for the first time over the SO, we assess the performance of the Cloud AeroSol Interacting Microphysics (CASIM) microphysics scheme (Field et al., 2023) in the Met Office Unified Model (MetUM) against new in situ aircraft and ground-based observations, as well as satellite observations. Our case studies are located where in situ observations are rare. Using case studies from February 2023, we focus on mixed-phased clouds and associated processes that impact the radiation balance over the SO. We aim to

- assess the representation of INP in the MetUM with CASIM and the impact on cloud representation and the surface cloud radiative effect;
- assess the impact of cloud droplet number on cloud representation in combination with INP changes;
- assess the impact of how well mixed the ice and liquid phase are within a grid-box on simulated cloud microphysical properties and on the surface cloud radiative effect.

An overarching aim is to improve the representation of clouds over the SO in models and assess the impact on the radiation balance.

SMITH ET AL. 2 of 22

2. Data and Methods

2.1. Aircraft Observations

Airborne measurements were collected using the British Antarctic Survey's Twin Otter MASIN research aircraft (Elvidge et al., 2015; Fiedler et al., 2010; King et al., 2008; Lachlan-Cope et al., 2016). A total of 20 flights (69 flight hours) were performed during the first Special Observation Period (SOP1) of the Southern Ocean Clouds (SOC) project in February 2023, based out of Rothera on the Antarctic Peninsula. The flights were performed over the Bellingshausen Sea and Marguerite Bay, targeting low-level stratiform, cumulus and frontal clouds. The flight plans were designed to capture both vertical profiles through the cloud layers, and straight and level legs flown above, below and through clouds. The overarching aim of SOC-SOP1 was to collect novel observations to inform the development of the representation of clouds and their radiative effect over the SO.

During SOC-SOP1, the Twin Otter MASIN research aircraft was fitted with a range of in situ aerosol and cloud microphysical instrumentation. A Passive Cavity Aerosol Spectrometer Probe (PCASP) provided particle numbers in 30 size bins across a diameter range of $0.1\text{--}3~\mu\text{m}$. Particle size distributions over the size range from 0.5 to 50 μm were also recorded using a cloud aerosol spectrometer (CAS, DMT Inc.; Baumgardner et al., 2001). The CAS sizing was calibrated by the manufacturer using polystyrene latex (PSL) spheres (<2 μm) and glass beads (>2 μm) (Baumgardner et al., 2014). Cloud droplets were measured by a cloud droplet probe (CDP-100, DMT Inc.; Lance et al., 2010) in the size range of 3–50 μm . Glass beads were used to determine the CDP's size bin centers and widths (Rosenberg et al., 2012). We use the CDP to compare with the MetUM.

The particle size distribution of larger hydrometeors were derived using the images from two optical array probes: a 2D-S (2D stereo, SPEC Inc.; Lawson et al., 2006) with a size range of 10–1,280 μ m (10 μ m pixel resolution) and a CIP-25 (cloud imaging probe, DMT Inc.; Baumgardner et al., 2001) with a size range of 25–1,600 μ m (25 μ m pixel resolution). The 2D-S and CIP-25 were fitted with anti-shatter tips to minimize ice break-up on their leading edges (Korolev et al., 2011). It should be noted that the CAS and CIP-25 are only available to the second half of SOP1 (from 12 February 2023 onwards) due to a technical issue. For the flights before 12 February 2023, we use the 2D-S, afterward we use the CIP-25. The 2D-S and CIP-25 images are processed with particles classified based on their geometry following Crosier et al. (2011). Particles smaller than ~80 μ m are too small to accurately determine their shape. For larger particles, three categories are derived, low irregular (LI), medium irregular (MI) and highly irregular (HI). LI are indicative of liquid drops and HI are indicative of ice crystals. The MI category is more ambiguous. However, during our case studies a negligible amount of the MI category is detected. We use 1 Hz data to calculate cloud property statistics. For details on which instruments were used, the statistical approach and how the observations are used for the model comparison see Section 3.4.

Static pressure and temperature were measured using standard aircraft sensors (King et al., 2008). The aircraft's highest quality hygrometer was not working during SOC-SOP1 and so we use data from a Vaisala Humicap sensor for humidity, which required calibration. For this, we use all coincident radiosonde observations from Rothera to apply an offset bias correction. There were six flights with a take-off time less than 2 hr after the 12 UTC radiosonde launches at Rothera. The take-off specific humidity profile was compared with the radiosonde specific humidity. All flights had a positive bias ranging from 0.1 to 0.7 g kg $^{-1}$. The humidity was reduced by the difference between the radiosonde and Humicap for that flight or the mean bias of 0.39 g kg $^{-1}$ as appropriate.

2.2. Ice Nucleating Particle Observations

Ice nucleating particles were measured from aerosol filters which were collected at a new aerosol lab on the East Beach of Rothera point (Lachlan-Cope et al., 2025). Whilst these measurements do not directly measure INPs at flight level, they are coincident in time and near the aircraft target area. Each filter was exposed to outside ambient air for 48 hr. The exposure time was chosen to balance sufficient time for detection and to allow for some temporal variability. A total of nine filters were obtained during SOC-SOP1 between the 4 and the 22 February 2023. These observations are discussed in Section 3.3. For the detailed methodology for deriving the temperature spectra for INP number concentration see supplementary information S1.

2.3. Satellite Observations

The Clouds and the Earth's Radiant Energy System (CERES) project provides satellite-based observations of Earth's radiation balance and clouds (Loeb et al., 2016; Wielicki et al., 1996). We utilize the CERES Single

SMITH ET AL. 3 of 22

21698996, 2025, 23, Downloaded from https://agupubs.onlinelibrary.wiley.com/doi/10.1029/2025JD044452 by British Antarctic Survey, Wiley Online Library on [27/11/2025]. See the Terms and Condit

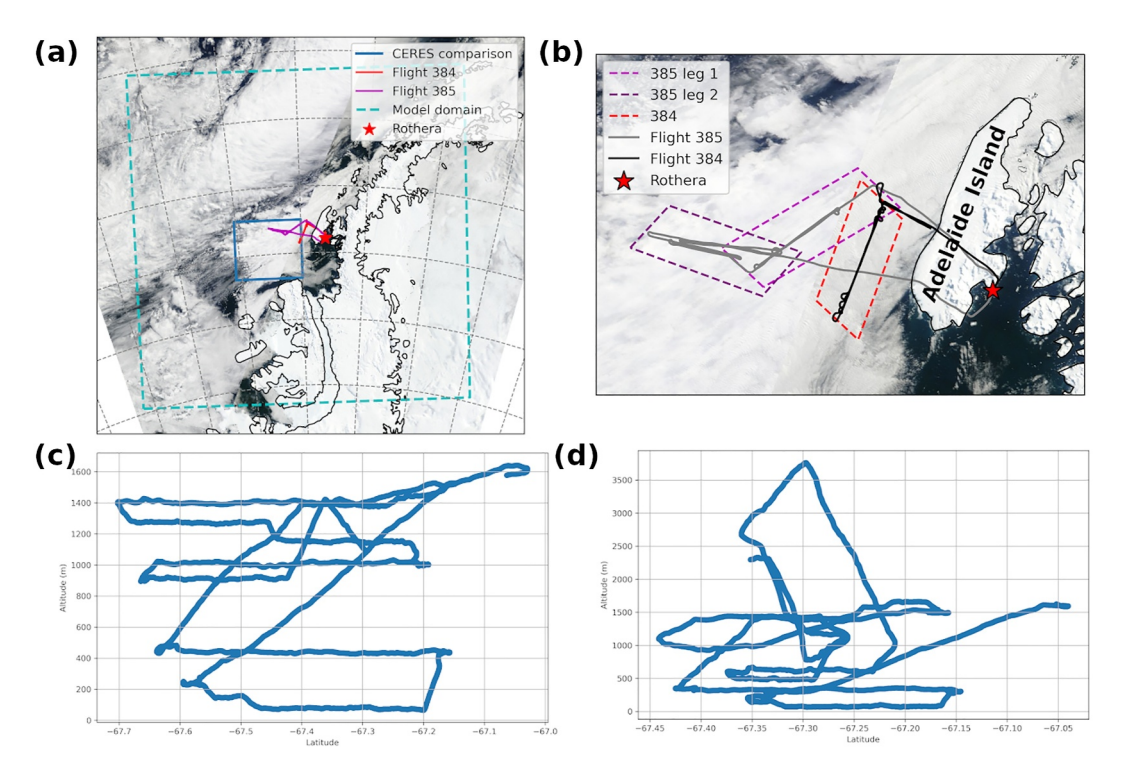


Figure 1. MODIS True Color image taken 6 February 2023 over the Antarctic Peninsula (a). Overlain are the model domain (dashed cyan box), Rothera station (red star), flight 384 track (red line), flight 385 track (purple line), and the area used to compare the model with satellite observations (blue box). The gridlines are spaced 2° latitude and 5° longitude. Image from NASA worldview (https://worldview.earthdata.nasa.gov/). A zoom in of the satellite image with the area used to compare model output to flight 384 (red dashed line) and the two legs of flight 385 (magenta and purple dashed lines) also illustrated (b). The flight track versus height for flight 384 (c) and for flight 385 (d).

Scanner Footprint (SSF) product, derived from MODIS aboard both the AQUA and TERRA satellites for top-of-the-atmosphere shortwave flux (TOA SW flux), TOA longwave (LW) flux and liquid water path (LWP). As this is an ungridded data set, we present statistics within the \sim 43,000 km² area show in blue in Figure 1a. Note this means the number of points used changes depending on the position of the box in relation to the swath, with more points at the swath center and less toward the edge, this may impact the data quality.

2.4. Case Studies

We primarily focus on a case study from SOC-SOP1 on the 6 February 2023 when measurements of low-level cloud ahead of an approaching front over the Bellingshausen Sea were made. Two back-to-back ~ 3.5 hr flights (flight 384 and 385) sampled the cloud characteristics and evolution over several hours. The cloud observed was between 500 and 1,750 m above sea level with temperatures between -4° C and -10° C. The path of the flights relative to the clouds observed from satellite can be seen in Figure 1b and the altitude and latitude of the flight tracks in Figures 1c and 1d. Flight 385 is split into two legs as each leg measured distinct types of cloud. The first leg, the north-east to south-west orientated section in Figure 1b, measured supercooled liquid cloud below 1,500 m. The second, east west orientated leg, measured the approaching frontal cloud up to 3,600 m with the aircraft unable to reach the cloud top. Note we also examined cases from the 7 and 19 February 2023 but for brevity, we only present a more limited analysis of these days. Table 1 summarizes the six flights used. These cases were selected as each had two flights with high quality data available and had minimal amounts of cloud above the sampled cloud to avoid the challenges and uncertainties caused by ice falling from upper cloud layers that weren't sampled.

SMITH ET AL. 4 of 22



Journal of Geophysical Research: Atmospheres

10.1029/2025JD044452

Table 1Flight Numbers, Date and Time of Flight Data Used and a Brief Summary of the Cloud Features Observed

Flight no.	Date (UTC)	Summary
384	6 February 2023 (14:00–16:15)	Stratiform supercooled liquid only cloud—pre front. Low pressure to the north west. Northerly flow near Adelaide Island.
385 leg 1	6 February 2023 (18:35–19:50)	Stratiform supercooled liquid only cloud—pre front. Low pressure to the north west. Northerly flow near Adelaide Island.
385 leg 2	6 February 2023 (19:50–21:15)	Mixed-phase frontal cloud. Low pressure to the north west. Northerly flow near Adelaide Island.
386	7 February 2023 (14:00–16:30)	Stratiform mixed-phase cloud—post front. Low pressure to the west. North westerly flow near Adelaide Island.
387	7 February 2023 (19:20–20:40)	Multilayered mixed-phase cloud. Low pressure to the west. North westerly flow near Adelaide Island.
396	19 February 2023 (15:30–18:00)	Multilayered mixed-phase cloud. Low pressure to the south west. Northerly flow near Adelaide Island.
397	19 February 2023 (20:00–22:00)	Patchy multilayered mixed-phase cloud. Low pressure to the south west. Northerly flow near Adelaide Island.

3. Modeling Approach

We use the Met Office Unified Model (MetUM) in its regional configuration with the CASIM double-moment microphysics scheme which has recently been implemented for operational purposes (Field et al., 2023). The CASIM microphysics scheme has rarely been evaluated over the Southern Ocean, so it is important to understand its performance in this region. Using a convection permitting configuration alleviates the uncertainties that arise from coupling the microphysics with a convection scheme and is similar to the regional UK focused configuration that is planned for operational forecasting (Bush et al., 2025).

3.1. Model Configuration

The MetUM version 13.0 is used, coupled to the Joint UK Land Environment Simulator to represent the land surface (Best et al., 2011). We use a 2.2 km resolution horizontal grid-length for a 500 by 500 grid point domain, with 90 vertical levels up to a model top at 40 km (20 levels below 1,500 m) and with the Regional Atmosphere and Land version 3 (RAL3) physics configuration. RAL3 builds upon the RA2M configuration (Bush et al., 2023), with the addition of CASIM (Field et al., 2023) and a new bimodal large-scale cloud scheme (Van Weverberg et al., 2021) in addition to other smaller changes (Bush et al., 2025). The limited area domain (shown in Figure 1) is driven by hourly data at the boundaries using output from a MetUM global atmosphere 8 (GAL8) simulation with a grid-length of 10 km. The model is initialized at 00 UTC 6 February 2023 from the global model analysis and runs for 24 hr. The first 12 hr are disregarded as the spin-up period. A similar approach is used for the 7 and 19 February 2023 cases.

The MetUM has previously been run and evaluated over the Antarctic Peninsula (e.g., Elvidge et al., 2015). The representation of clouds and their radiative impact on the surface melt of the Larsen C ice sheet were assessed in Gilbert et al. (2020) using the earlier Regional Atmosphere and Land version (RA1) configuration which uses the MetUM's single-moment scheme (Wilson & Ballard, 1999). Whilst changes to the microphysics and large-scale cloud schemes offered some improvements, some cloud phase biases remained, Gilbert et al. (2020) highlighted that further development and moving to a double-moment scheme was required. More recently, the implementation of RAL3 was compared to RA2M, highlighting improvements in the representation of a snowfall event over coastal Antarctica but many deficiencies remain with the representation of INP a key challenge (Pei et al., 2025). In separate recent studies, the MetUM with CASIM has been configured over coastal Antarctica also highlighting significant errors in simulated cloud and surface radiation balance (Hansen et al., 2024; Price et al., 2025).

SMITH ET AL. 5 of 22

Table 2 MetUM Experiments With the Ice Nucleating Particle Parametrization (INP), Fixed Cloud Droplet Number (Nd), and Mixed-Phase Overlap Factor (MPOF) Used

Experiment name	INP curve	$Nd (cm^{-3})$	MPOF
Control	Cooper	150	0.5
SOC	SOC	150	0.5
V21	V21	150	0.5
Nd75	SOC	75	0.5
MPOF0	SOC	75	0
MPOF1	SOC	75	1

MetUM with CASIM has been configured and has shown to provide more realistic simulations than the current operational single-moment scheme (Field et al., 2023). We use the proto-operational configuration as our control (Field et al., 2023). Whilst CASIM can be configured to be coupled with an aerosol field in the MetUM, here we use it in its operational configuration with a fixed droplet number profile and a temperature dependent heterogeneous ice nucleation scheme. Importantly, CASIM contains a secondary ice production scheme that represents the Hallet-Mossop rime splintering effect (Hallett & Mossop, 1974) which is active between -2.5°C and -7.5°C and is implemented without any liquid or solid water content thresholds. CASIM also contains the Bigg (1953) heterogeneous freezing of raindrops into graupel. For more details see Field et al. (2023). Details on the parametrizations of the processes examined are described in Section 3.3.

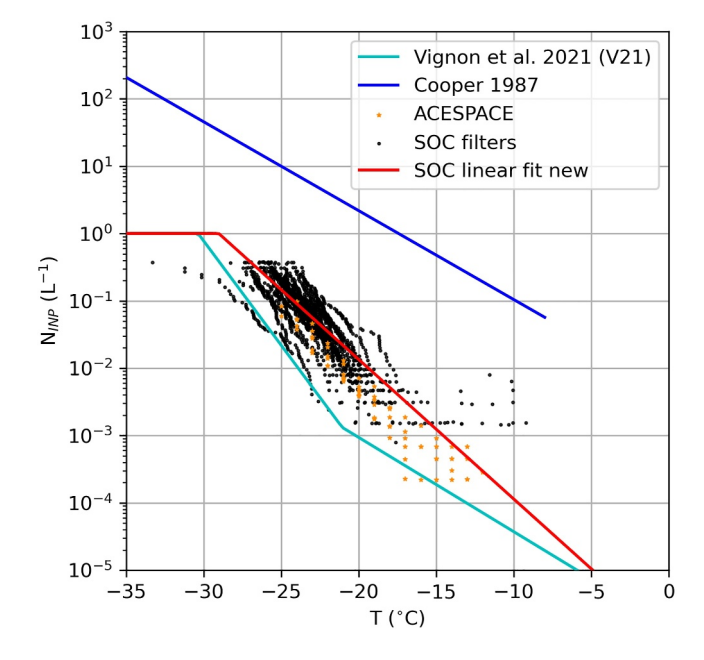


Figure 2. Ice Nucleating Particle concentrations (L^{-1}) as a function of temperature. Observations from filters taken at Rothera during the SOC-SOP1 flying campaign (black dots) and from ACESPACE during February in the vicinity of Rothera (orange stars). Overlaid are parametrization relationships from Cooper (1987, blue) the MetUM's default, from Vignon et al. (2021, cyan); and an SOC parametrization based on a fit to our observations (red).

3.2. Microphysics Parametrization

CASIM is a double moment microphysics scheme that contains five hydrometeor species (liquid cloud droplets, rain, ice, snow and graupel) with prognostic number concentration (N) and mass mixing ratio (q). Here the cloud droplet number, N_d , is prescribed. CASIM has been designed to be flexible and configured with a range of complexity. It was first introduced and developed in the Kinematic Driver model (Hill et al., 2015; Miltenberger et al., 2020; Shipway & Hill, 2012) and later in a Large Eddy Simulator (e.g., Hawker et al., 2021; Poku et al., 2021). Research configurations of CASIM within the MetUM have been developed to investigate various cloud types (e.g., Finney et al., 2025; Grosvenor et al., 2017; Huang et al., 2025; McCusker et al., 2023; Miltenberger et al., 2018; Price et al., 2025) and can include aerosol-cloud interactions. Recently, an operational version of the

3.3. Model Experiments

We run six sensitivity tests (Table 2) focusing on the parametrization of three key mixed-phase microphysical processes namely, the heterogeneous ice nucleation scheme, the cloud droplet number concentration and the mixed phase overlap factor (MPOF).

The heterogeneous ice nucleation scheme controls the initial production of ice between 0°C and -38°C, that is, the primary ice production. The default setting is to nudge the cloud ice number concentration to the values suggested by Cooper (1987), below -8°C, as a function of temperature. These values are known to be too large for the SO (e.g., McCluskey et al., 2018; Vergara-Temprado et al., 2018; Vignon et al., 2021) and compared to those observed at both Rothera during SOC-SOP1 and during the ACESPACE research cruise (Tatzelt et al., 2020) in February 2017 when it was within our model domain (Figure 2). The Cooper (1987) scheme is used in various models, for example, in the Morrison et al. (2005) microphysics scheme used in gSAM (e.g., Atlas et al., 2022) and in some configurations of WRF (e.g., Listowski & Lachlan-Cope, 2017). We perform two sensitivity tests using temperature dependent schemes suitable for the SO; one scheme derived for the Mawson Station in East Antarctica (Vignon et al., 2021, V21) and another derived using SOC observations during SOP1. The SOC fit was derived in an equivalent manner to Vignon et al. (2021) including limiting the INP concentration to $1 L^{-1}$ below -28° C in line with the DeMott et al. (2010) parametrization and observations during CAPRICORN (McCluskey et al., 2018). Both Antarctic curves represent INP concentrations that are orders of magnitude smaller than the Cooper curve, and other common INP parametrizations (e.g., DeMott et al., 2010).

The default cloud droplet number concentration was halved, from 150 to 75 cm⁻³, to match observations during SOC-SOP1 (Figure 3). Note that the clouds observed range from stratiform, cumulus and frontal including both

SMITH ET AL. 6 of 22

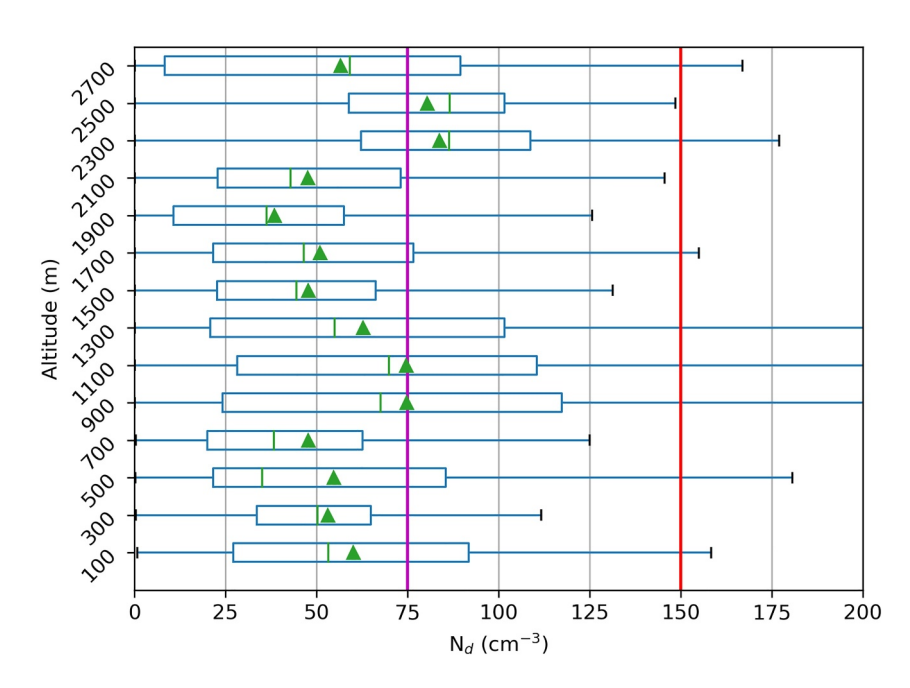


Figure 3. In-cloud CDP droplet number concentration (cm⁻³) in height bins for all 20 SOC-SOP1 flights. The triangles show the bin mean and the green line the median. The red and purple lines show the control and experimental model settings for N_d . All bins have at least 300 points.

precipitating and non-precipitating clouds and cover supercooled liquid, mixed-phase and ice only clouds. Previous studies have also shown that droplet numbers over the Southern Ocean are lower than those elsewhere. For example, median droplet number concentrations of 124 and 155 cm⁻³ (in 2010 and 2011) were found to the west of the Antarctic Peninsula; and 103 and 192 cm⁻³ (in 2010 and 2011) were found to the east (Lachlan-Cope et al., 2016). Over the Weddell Sea campaign median droplet number concentration of 113 cm⁻³ was found (O'Shea et al., 2017) and median values of 69 cm⁻³ over the SO in the area between 45° to 62°S and 132° to 164°E (McCoy et al., 2020). As a result, other modeling studies have chosen to reduce the droplet number (e.g., Young et al., 2019) with the Polar WRF configuration of the Morrison et al. (2005) scheme set up with a reduced droplet number concentration of 50 cm⁻³ rather than 250 cm⁻³ (Xue et al., 2022). This experiment allows a comparison of the impact of uncertainties in the cloud droplet number compared to those of primary ice production.

The final set of experiments change the mixed-phase overlap factor (MPOF) which represents how well-mixed horizontally the liquid and ice phases are within a grid-box (See Field et al., 2023 for formulation). The liquid and frozen cloud fractions are calculated by the large-scale cloud scheme (Van Weverberg et al., 2021). Where a gridbox has both a liquid and frozen cloud fraction it is necessary to make assumptions on how they overlap. MPOF controls this overlap. Figure 4 illustrates how well mixed the clouds are within a grid-box for a given MPOF and several liquid and frozen fractions. An MPOF value of 1 means the two phases are fully overlapped representing genuinely mixed-phase cloud (Figure 4c). A value of 0 means they are minimally overlapped representing conditionally mixed-phase cloud (Figure 4a). Cloud microphysical interactions between liquid and frozen particles can only occur in the mixed-phased fraction of the grid-box by scaling the microphysical process rates by the mixed-phase fraction. The MetUM default is MPOF = 0.5 (Figure 4b), but this setting has not previously been examined in depth to determine if this is appropriate. In parallel with our study, an observational analysis examining aircraft data from multiple field campaigns has been performed to constrain this value (Evans et al., 2025). They found an average value of approximately 0.8 but measurements show this varies in natural clouds. Whilst this parameter is specific to the MetUM CASIM configuration, other models have to confront this physical constraint using similar approaches. For example, by adjusting the rate of the WBF process, in CAM5 (Tan & Storelymo, 2016) and CAM6 (Gettelman et al., 2020), where reducing the efficiency of the WBF process by 75% resulted in an increase in LWP, increase in IWP and consequently a reduction in shortwave cloud radiative effect by 10 W m⁻². Here, we examine the sensitivity of the model to MPOF (which effects all mixedphase processes) to understand how sensitive the model cloud and radiation balance could be to this

SMITH ET AL. 7 of 22

21698996, 2025, 23, Downloaded from https://agupubs.onlinelibrary.wiley.com/doi/10.1029/2025JD044452 by British Antarctic Survey, Wiley Online Library on [27/11/2025]. See

Figure 4. Schematic of the mixed-phase overlap factor (MPOF) parametrization used in CASIM. The liquid droplets are represented with blue circles and ice crystals with purple hexagons. The columns show a() MPOF = 0 (b) MPOF = 0.5; (c) MPOF = 1 with each showing a different cloud fraction example: (i) a liquid and ice fraction of 0.5; (ii) a liquid fraction of 0.5 and ice fraction of 0.25; (iii) a liquid fraction of 0.75 and ice fraction of 0.5.

parametrization in comparison to the other processes. We perform two sensitivity experiments, one with MPOF = 0 and one with MPOF = 1 in a similar approach to Van Weverberg et al. (2023). They found, for mixed-phase clouds in Norway, that the MetUM was more sensitive to microphysical processes, such as riming, than MPOF as their simulations were dominated by fully overcast conditions.

3.4. Model Comparison Methodology

To compare the model with observations we perform statistical binning both spatially and temporally to avoid issues related to sampling differences. For the aircraft observations, we take the entire flight and bin it into 200 m height bins calculating the mean and 10th and 90th percentiles. Only bins with at least 10 measurements are kept, with some bins that contain level flight legs, having up to 1,500 measurements. For the model, we take the area around the flights shown in Figure 1 and calculate the arithmetic mean over this area for the duration of the flight or flight leg.

For the microphysics comparison we use a threshold to determine if the observations/model data points are incloud and here only in-cloud values are analyzed. Note liquid and solid as well as mass and number are treated separately. For example, the mass can be greater than the mass mixing ratio threshold and therefore appears in figures where mass is shown, but the number concentration could be less than the number concentration threshold in which case a figure of number concentration would not show any in-cloud values (even when mass is shown). The thresholds to determine if a measurement or model grid-box is in cloud are

- Mass >0.005 g kg⁻¹ for each individual hydrometeor species to compare hydrometeor mass between the model and observations. The CDP is used for liquid and the 2D-S HI for solid.
- Number >0.2 L⁻¹ for comparing modeled snow number concentration with the 2D-S HI. This value is constrained by the limitations of the 2D-S. Note that for the droplet number comparison, the in-cloud model concentration is fixed so no number threshold is required; from the CDP we use the same mass threshold to determine an in-cloud value.

The model outputs grid-box mean hydrometeor species to calculate in-cloud values; so, the species must be converted to in-cloud values by dividing by the grid-box cloud fraction. Note if the grid-box cloud fraction is less than 0.05 then that grid point is regarded as 'cloud free' and is removed from the analysis. The choice of this value has been tested and has a negligible impact on results.

The 2D-S measures all particles in the size range so to distinguish ice from liquid, we use the HI (highly irregular) category and compare this to the modeled snow. We also inspected all images to remove any period of mis-diagnosed out of focus droplets that were flagged as HI particles. From the highly irregular category the mass is calculated using the same mass-diameter relationship used for snow in CASIM (Cotton et al., 2013). The mass (m) diameter (D) relationship takes the form $m = cD^d$ where c = 0.026 and d = 2. There are large uncertainties associated with mass diameter relationship for snow due to the assumptions about the particle habit and density. This version is chosen to remove any differences, caused by the mass diameter relationship, between the model and observations.

SMITH ET AL. 8 of 22

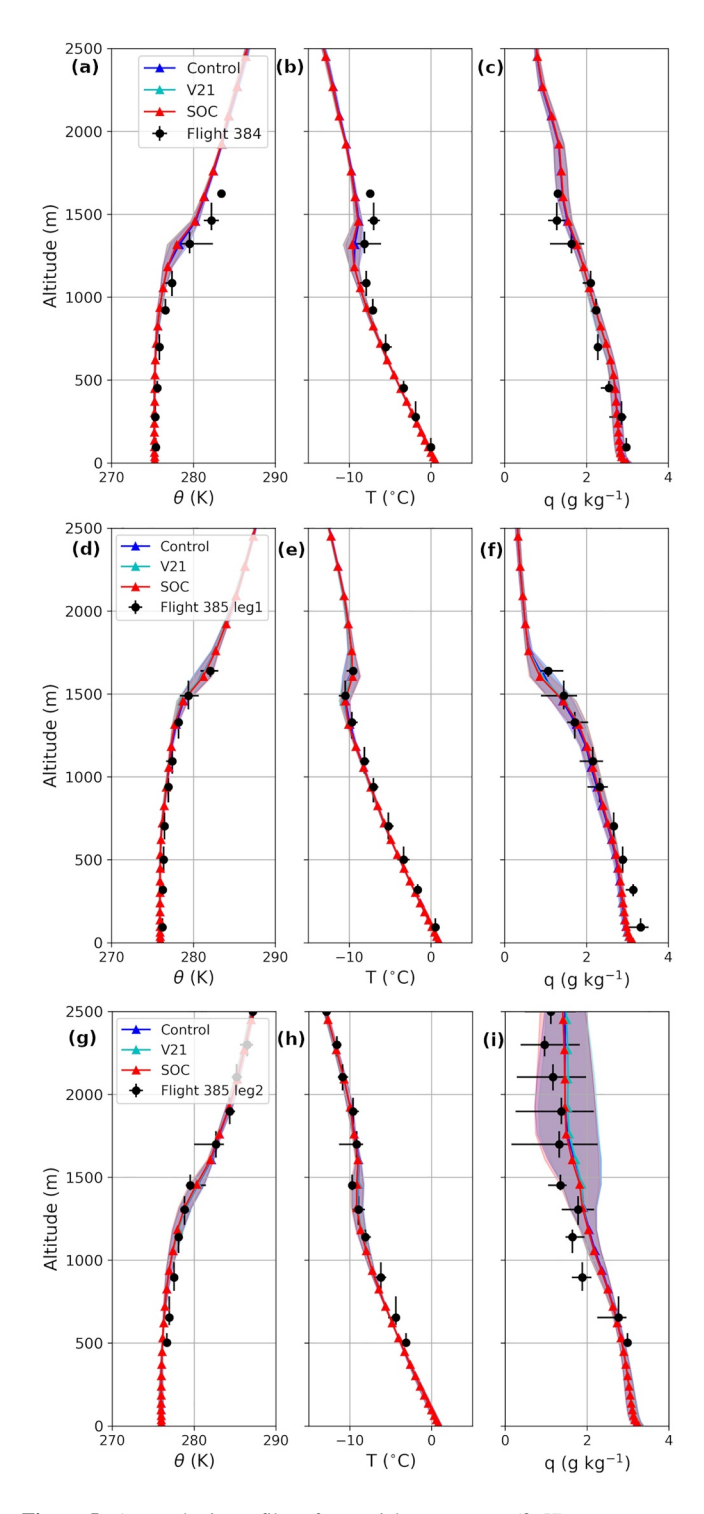


Figure 5. Atmospheric profiles of potential temperature $(\theta; K)$, temperature $(T; {}^{\circ}C)$ and corrected specific humidity $(q; g kg^{-1})$ showing binned aircraft observations (black) with the dot showing mean and the bar showing the 10th and 90th percentiles both for the variable in the x direction and altitude in the y direction and model output from the Control (blue), V21 INP (cyan), SOC INP (red) simulations, for flight 384 (top) and flight 385 leg 1 (middle) and flight 385 leg 2 (bottom) with the line showing the mean and the shading \pm one standard deviation.

4. Results

4.1. Meteorological Assessment

First, the model is compared with the observed temperature and humidity profiles from each flight. In general, the low-level meteorology is simulated well (Figure 5). However, the model is unable to resolve the strength of the temperature inversion at the top of the boundary layer which results in the model temperatures being too low by about 2°C at an altitude of 1,500 m during flight 384. The temperature inversion differences could be related to inadequate vertical resolution or the cloud-top turbulence parametrization. A comparison to radiosondes launched at Rothera at 12 UTC give a similar correspondence (not shown). However, later during flight 385 the cloud top inversion was simulated well in the model. During the second leg of flight 385 there is a noteworthy specific humidity bias which is addressed further in Section 4.2.2. However, note this error is within the 18% error of the uncorrected humidity observations so this difference could be attributed to the observational error. Note there is little difference between the sensitivity tests. In short, the model is able to reproduce the temperature and humidity well during these flights and also the other cases examined. More broadly, the simulations capture the synoptic-scale circulation reasonably well.

4.2. Microphysics Assessment

4.2.1. Flight 384

Figure 6 shows both the in-cloud (see Section 3.4 for definition) mass mixing ratio and number concentration observed and for the five hydrometeor species in CASIM averaged over the area of the flight 384 track. In the main cloud deck, no simulation produces enough liquid water content (LWC). There is very little sensitivity between the simulations, the lines in Figure 6 overlap. This limited sensitivity is due to the small amount of ice phase hydrometeor species and small ice cloud fraction, meaning any changes to the INP and MPOF have a limited effect. Indeed, during this flight, there were no highly irregular particles measured by the 2D-S. Therefore, the simulations with snow are overproducing ice phase hydrometeors compared to the observations. The observed cloud droplet number concentration falls between the 75 and 150 cm⁻³ values used in the model tests above 800 m and is less than 75 cm⁻³ below 800 m. Reducing Nd increases the rain concentration and mass as a result of the additional autoconversion, which is a function of Nd to the power -1.79, as parametrized by Khairoutdinov and Kogan (2000). There is limited impact from MPOF as the frozen cloud fraction is close to zero. However, the MPOF1 simulation is the only simulation that produces enough snow to meet the in-cloud threshold for snow, highlighting the impact of the phase overlap. Note there is not sufficient ice mass or graupel mass and concentration to be deemed as in-cloud during this flight.

4.2.2. Flight 385

Comparing the control simulation, during the first leg of flight 385, with the observations, the LWC compares well, particularly below 1,300 m. Above 1,300 m the simulated LWC is too high. The observed cloud droplet number concentration is lower than the first flight (Figure 7) and matches closely to the Nd75 simulations (and the campaign average).

SMITH ET AL. 9 of 22

21698996, 2025, 23, Downloaded from https://agupubs.onlinelibrary.wiley.com/doi/10.1029/2025JD044452 by British Antarctic Survey, Wiley Online Library on [27/11/2025]. See the Terms and Conditions

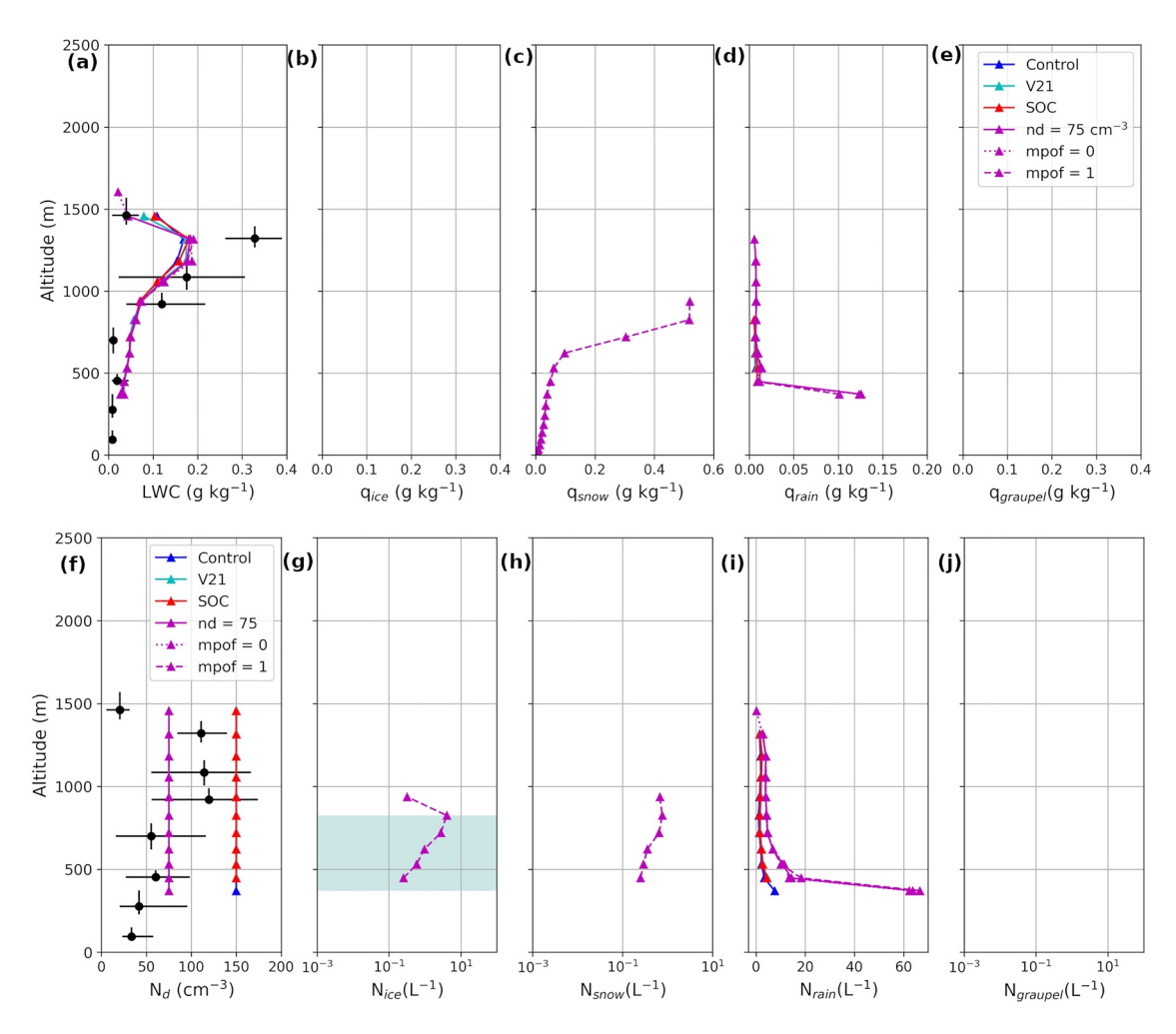


Figure 6. Binned microphysical aircraft observations (black) with the dot showing the mean and the bar showing the 10th and 90th percentiles both for the variable in the x direction and altitude in the y direction, and model output for Control (blue), V21 INP (cyan), SOC INP (red), droplet number concentration Nd of 75 cm $^{-3}$ (magenta), MPOF = 0 (magenta dotted) and MPOF = 1 (magenta dotted) simulations. Variables shown are in-cloud mean liquid, ice, snow, rain and graupel mass mixing ratio (top, g kg $^{-1}$) and number concentration (bottom, cm $^{-3}$ for liquid and L $^{-1}$ for all other species) for flight 384. The teal shading indicates a layer with temperatures between -2.5° C and -7.5° C where the Hallet-Mossop process is active.

Again, the aircraft measurements show that these clouds were dominated by supercooled liquid water, without any measurable ice by the 2D-S. Across all the experiments the model simulates too much snow. In the high-lighted Hallet-Mossop temperature range the model produces high ice concentrations due to secondary ice production. Note that the simulated ice number concentration exceeds the number threshold, but the ice mass does not reach the mass threshold, as the modeled ice is small in size, hence only ice number is shown in Figure 7. The control experiment, with the Cooper (1987) INP scheme, produces the most snow and ice and therefore the largest snow error. Reducing the INP leads to a reduction in ice number concentrations, as primary ice production produces the ice hydrometeor category. These are small ice particles that can grow to snow, hence the higher snow mass and number in the control simulation compared to the V21 and SOC simulations. In the Hallett-Mossop temperature range the simulations of ice are closer to each other, with the control around one order of magnitude larger in terms of ice number despite having three orders of magnitude higher INP, highlighting that the secondary ice production in the model in this temperature range is having a significant impact on the ice and snow concentrations. The reduction in ice concentrations in the V21 and SOC simulations results in higher liquid water concentration as a result of the reduction of riming.

The Nd75 simulation (Solid purple lines) has an increased rain concentration and mass in both flights. The additional rain results in the larger snow mass via riming. The secondary ice is a function of the snow riming rate

SMITH ET AL. 10 of 22

21698996, 2025, 23, Downloaded from https://agupubs.onlinelibrary.wiley.com/doi/10.1029/2025JD044452 by British Antarctic Survey, Wiley Online Library on [27/11/2025]. See the Terms

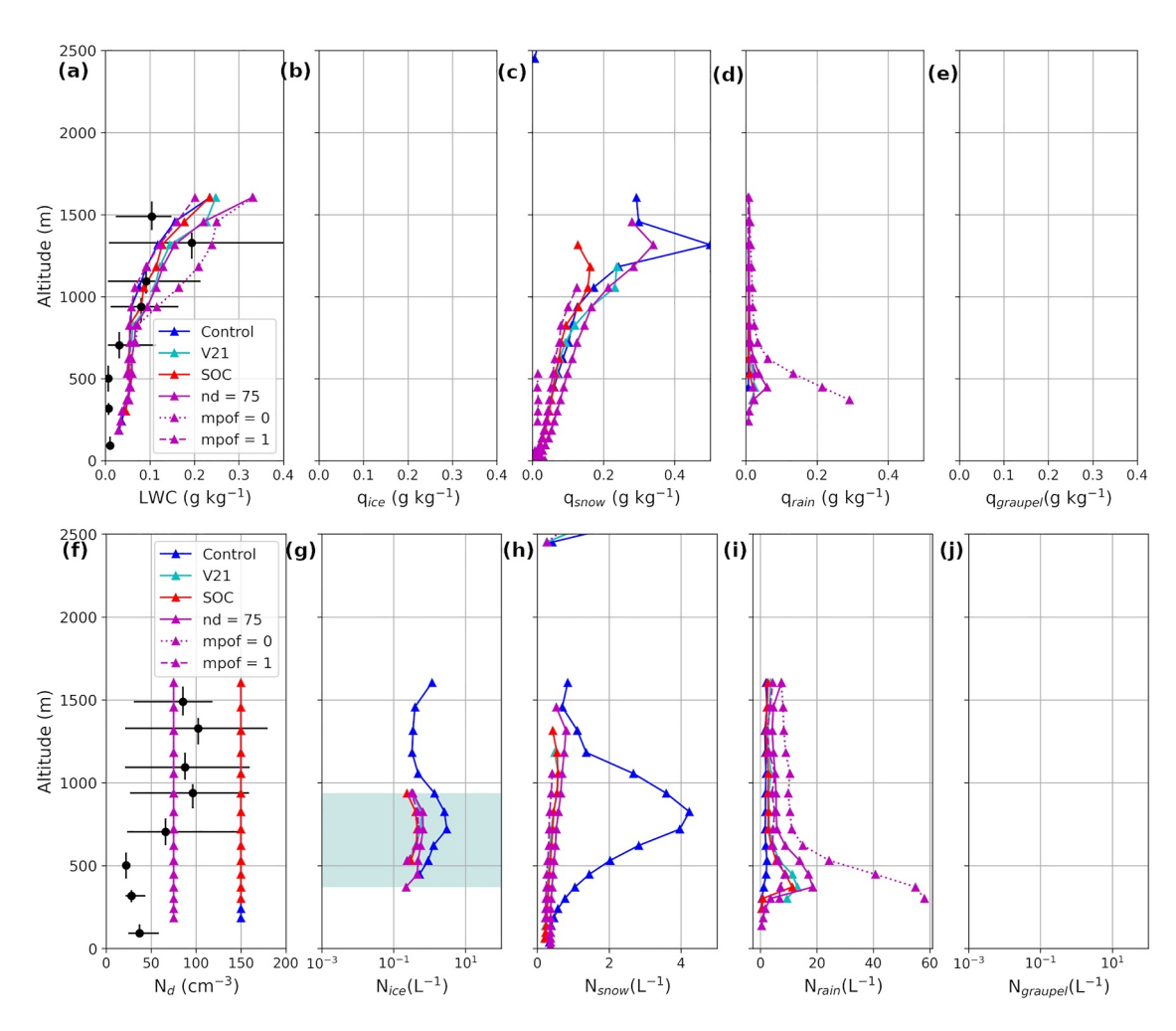


Figure 7. Binned microphysical quantities, as Figure 6, but for flight 385 leg 1.

(Field et al., 2023) and thus there is also a small increase in the ice number concentration in the reduced Nd simulation.

The MPOF has a large impact on the LWC, with zero overlap (MPOF0) giving an increase in LWC of up to $0.1~{\rm g~kg^{-1}}$, larger than caused by either reducing the droplet number or the INP. In the MPOF0 simulations less liquid is converted to ice resulting in lower snow mass and number. Note that unlike flight 384 the liquid and frozen fractions are between 0 and 1. For example, at 1,000 m in the control there is an average liquid cloud fraction of 0.5 and a frozen cloud fraction 0.25 (see Supporting Information S1 for more information) which is in the regime shown in Figure 4ii illustrating the cause of the sensitivity. The large sensitivity to MPOF highlights the important role it can have in modulating the simulated hydrometeor species and demonstrates that accurately representing the phase overlap needs to be considered to improve simulations of mixed-phased cloud in partially cloudy situations.

The second cloud leg of flight 385 sampled low-level cloud with snow falling into the cloud from an approaching deck of frontal cloud above (Figure 8). The difference in cloud morphology, compared to the other two legs, highlights some additional impacts of the different processes considered.

Overall, the simulations produce too much liquid and snow compared to the observations. The simulated mass and number concentration of snow is higher than observed in all experiments. For example, at 2,500 m the observed mass mixing ratio was $0.03~{\rm g~kg^{-1}}$ and the simulations ranged from 0.24 to $0.26~{\rm g~kg^{-1}}$. Similarly, at 2,500 m the observed snow concentrations (HI particles from the 2-DS) was $0.79~{\rm L^{-1}}$ and the simulations ranged from 32 to $37~{\rm L^{-1}}$. The profiles suggest that too much snow is falling into the low-level clouds from higher clouds above. The difference could be a result of the front progressing slightly earlier in the model, uncertainties in the snow fall

SMITH ET AL. 11 of 22

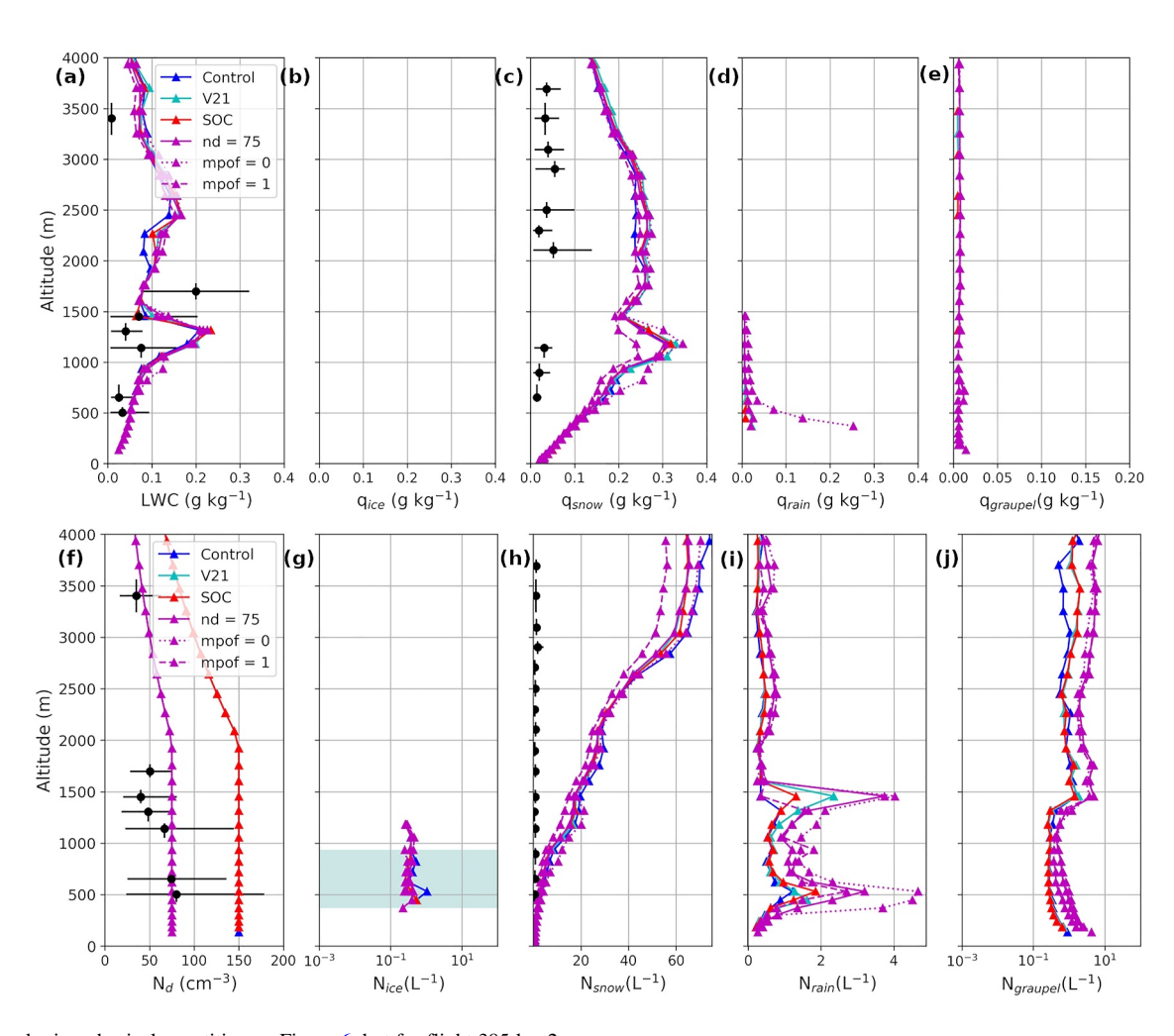


Figure 8. Binned microphysical quantities, as Figure 6, but for flight 385 leg 2.

speed or other model parametrizations such as turbulence in the free troposphere. In addition, during this period the model humidity was too high, likely caused by the sublimation/evaporation from too many falling hydrometeors or alternatively, there could be less snow observed because the atmosphere is drier leading to a higher sublimation rate.

These low-level clouds are less sensitive to the parametrizations tested than other cases with a few noteworthy differences. They are largely insensitive to the INP as the cloud top temperature of the higher frontal clouds, that are seeding the observed clouds, is lower than -38° C so homogeneous freezing is the dominant ice source. The simulations with reduced Nd have more rain and more graupel because of the heterogeneous freezing of rain previously discussed. The MPOF sensitivity tests show an inverse relationship during this leg compared to the other two legs. Similar to leg 1, the average liquid and frozen cloud fractions at 1,000 m are 0.4 and 0.6 respectively so again the simulate cloud is in the regime illustrate in Figure 4ii necessary to see the sensitivity to MPOF. The lower MPOF value has more snow which is likely caused by more liquid (0.034 g kg⁻¹ compared to 0.032 g kg⁻¹) having been lifted to the homogeneous freezing level as less liquid has been converted to ice at lower levels. After the additional liquid reaches the homogeneous freezing level, it can freeze and fall out to the lower levels as seen in Figure 8 resulting in additional snow at the lower levels. Note that, similar to the other legs the impact of SIP can be seen in the ice number concentrations.

In summary, the comparison between the model and aircraft data shows the model produces a reasonable amount of cloud liquid but too much snow compared to the observations. A reduction in INP reduces the snow mass and number but a high bias remains. A reduction in droplet number, closer to that observed, results in a higher rain mass and number that is then converted to additional snow and graupel (i.e., not observed). An increase in MPOF leads to

SMITH ET AL. 12 of 22

21698996, 2025, 23, Downloaded from https://agupubs.onlinelibrary.wiley.com/doi/10.1029/2025JD044452 by British Antarctic Survey, Wiley Online Library on [27/11/2025]. See the Terms and Conditions

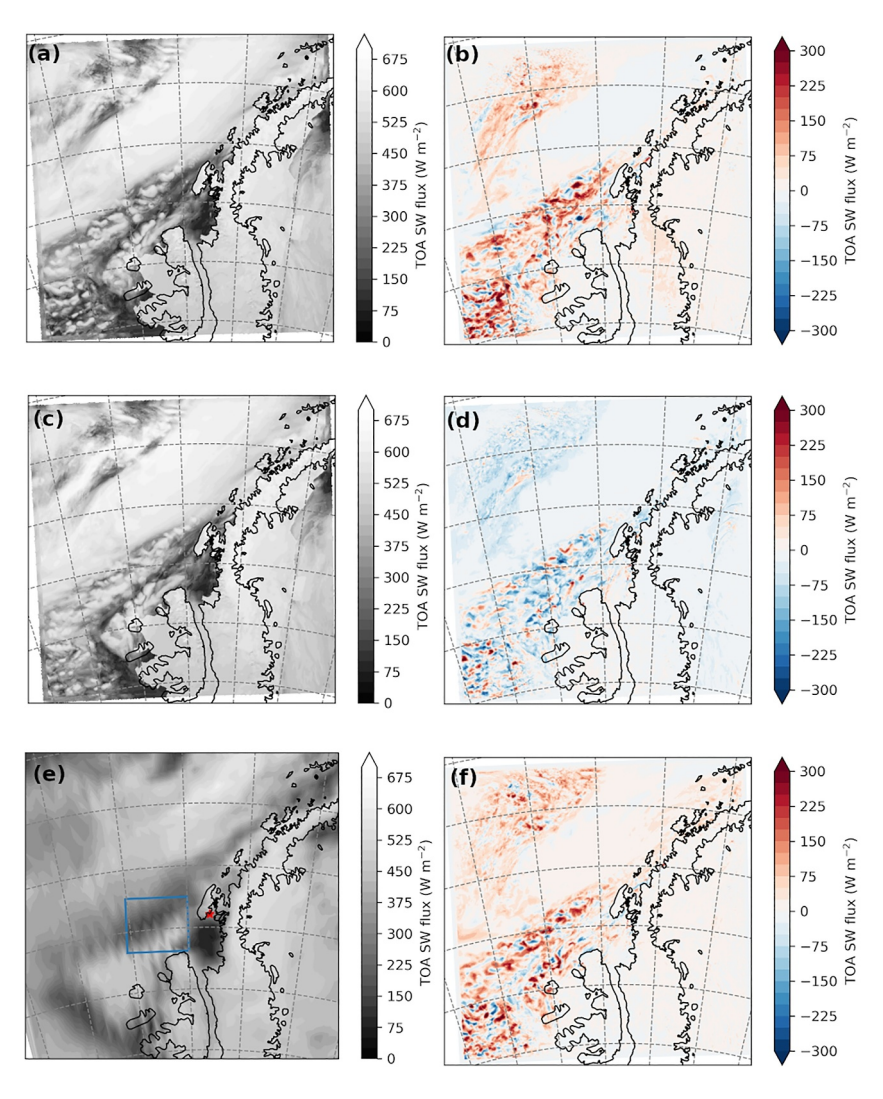


Figure 9. Top of the Atmosphere Shortwave flux (W m^{-2}) from the control (a) and SOC experiments (c), CERES (e); and the difference between the SOC and control (b), the Nd = 75 and SOC (d), and the MPOF0 and MPOF1 experiments (f), at 1800 UTC 6 February 2023.

more snow mass and number, and reduced LWC in the low-level cloud legs, but the inverse is seen in the leg with the deeper cloud above that has a top colder than the -38° C needed to trigger homogeneous freezing in the model. Additional assessments of the model microphysics for other flights are in Text S3 in Supporting Information S1.

4.3. Evaluation Against Satellite Products

Comparing the model TOA shortwave flux with that from satellite (Figures 9 and 10) shows the model replicates the broad structure of the observed cloud with the front to the west and the low-level cloud close to Adelaide Island (Figure 1). The low-level cloud in the model is more broken than observed (compare Figures 1 and 9) with the observations detecting LWP over the whole area while the model produces LWP close to zero for some grid-boxes (Figure 10). Although the model does capture the clear conditions south of Adelaide Island.

Comparing the different sensitivity tests, the impact of each experiment is mostly confined to the low-level cloud, rather than the frontal cloud, consistent with the sensitivity to the different hydrometeor species discussed in Section 4.2. The reduced INP (SOC - Control) results in brighter and broader clouds (Figure 9). Consequently, leading to higher TOA SW flux with the median increasing by around 50 W m $^{-2}$ consistent with less ice and snow (although slightly higher IWP in Figure 10) and greater liquid (Figures 6 and 10) by approximately 0.03 kg m $^{-3}$. The reduced primary ice production results in less snow fallout, allowing a greater cloud extent with greater LWC

SMITH ET AL. 13 of 22

21698996, 2025, 23, Downlo

ded from https://agupubs.onlinelibrary.wiley.com/doi/10.1029/2025JD044452 by British Antarctic Survey, Wiley Online Library on [27/11/2025]. See the Terms and Condit

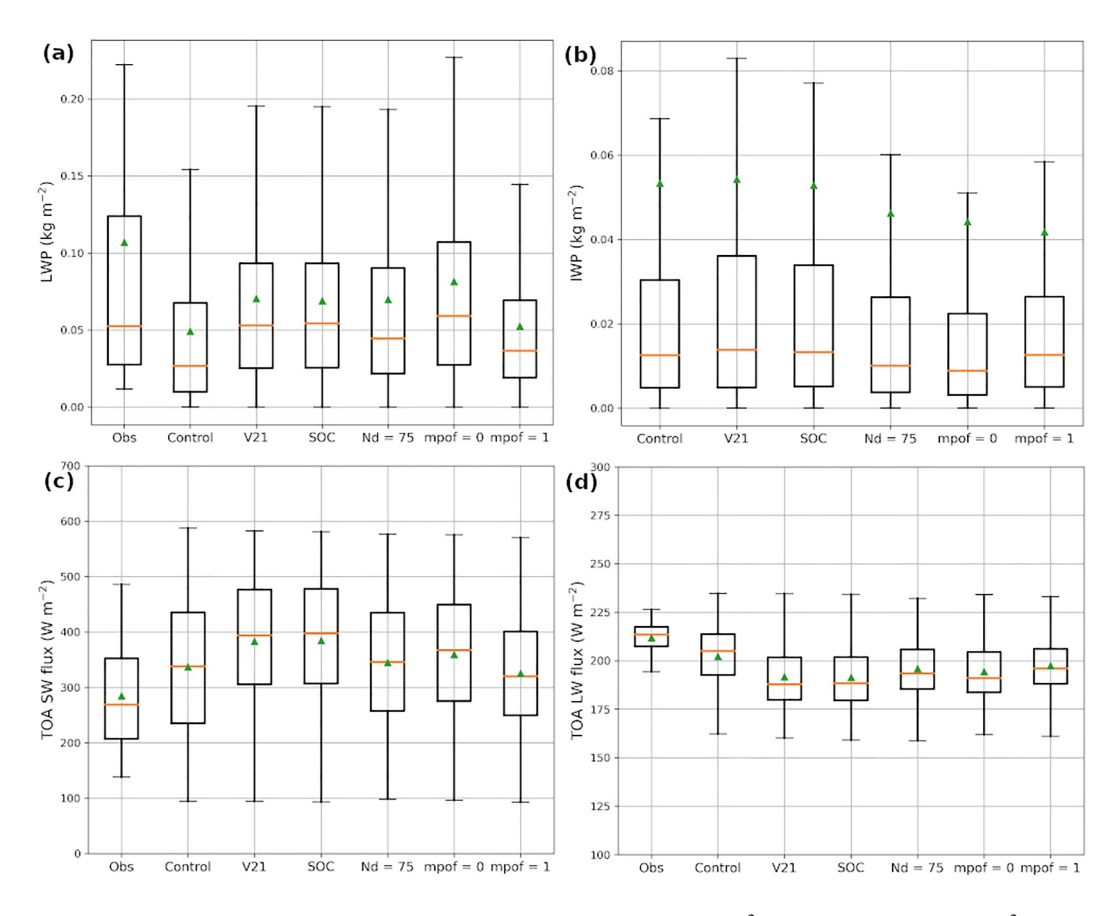


Figure 10. CERES (except IWP) and MetUM output for liquid water path $(a, kg m^{-2})$ and ice water path $(b, kg m^{-2})$ Top of the Atmosphere Shortwave flux $(c, W m^{-2})$, Top of the Atmosphere Longwave flux $(d, W m^{-2})$, over the area of the blue box in Figure 1 at 18:00 UTC 6 February 2023. Orange line indicates the median, the box the interquartile range and the green triangles the mean.

and hence a higher albedo. Even though the SOC LWP is higher and closer to observed LWP than the control LWP (Figure 10), the increased TOA SW and reduced TOA LW (~10 W m⁻²) are further from the satellite measurements. Note there are almost negligible differences when comparing the SOC and V21 simulations in terms of IWP, LWP, TOA SW flux, and TOA LW flux.

In contrast, the reduced Nd (Nd75–SOC) results in a reduction in TOA SW flux by a similar amount (Figures 9 and 10). The reduction in TOA SW flux is from a combination of the albedo effect, less droplets result in larger less reflective droplets reducing the cloud albedo and being more broken likely caused by the increased rain and snow seen in Section 4.2. Again, the median TOA SW flux change is about 50 W m $^{-2}$ (Figure 10). The impact on the TOA LW flux (\sim 10 W m $^{-2}$) is caused by the more broken cloud and hence higher LW from the warmer sea surface. There is also a reduction in the LWP in the Nd75 run (Figure 10) compared to SOC, although this is smaller than the impact of the reduced INP. The reduced Nd experiment brings the TOA SW flux closer to observed, highlighting how changes in Nd and INP over the Southern Ocean can partially compensate.

Examining the sensitivity to MPOF (MPOF0–MPOF1) illustrates a similar magnitude increase in TOA SW flux-broadly similar to the other experiments (Figures 9 and 10). Increased MPOF results in lower LWP by approximately 0.03 kg m $^{-3}$ and to a lesser extent increased IWP, indicative of liquid clouds glaciating and consistent with the reduced LWC seen in Section 4.2. These phase differences result in lower TOA SW fluxes (\sim 40 W m $^{-2}$) and higher LW fluxes (\sim 5 W m $^{-2}$) in the MPOF1 simulation. The significant impact on the TOA fluxes further highlights the need to better constrain MPOF.

Figure 11 summarizes cloud representation impacts on TOA radiative fluxes via differences in the simulated fluxes for the different sensitivity experiments and across several case studies. The colors show results for eight

SMITH ET AL. 14 of 22

21698996, 2025, 23, Downloaded from https://agupubs.onlinelibrary.wiley.com/doi/10.1029/2025JD044452 by British Antarctic Survey, Wiley Online Library on [27/11/2025]. See

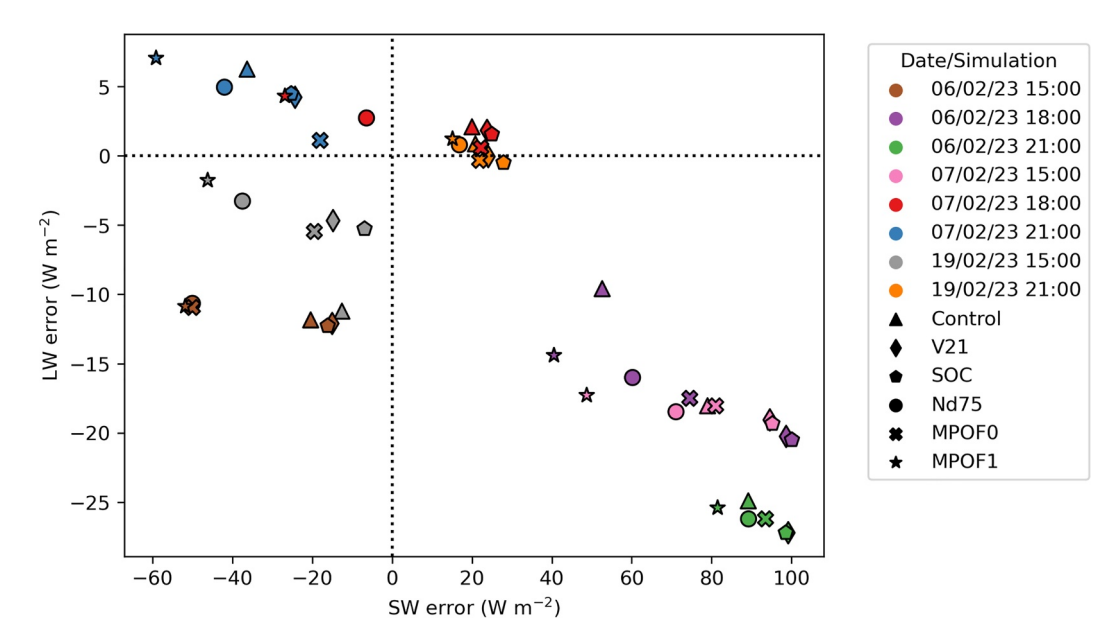


Figure 11. Summary of the cloud representation impacts on radiative fluxes over 8 times. The axes show the difference between simulated and CERES TOA longwave and shortwave flux medians within the blue box (see Figure 1). The colors indicate the time of comparison and the marker style the sensitivity test: control (triangles), V21 (diamonds), SOC (pentagons), Nd75 (circles), MPOF0 (crosses), and MPOF1 (stars).

satellite passes including the 7 and 19 February case studies. The purple symbols illustrate the results of Figure 10. Recall brief summaries of all the flights are in Table 1.

The first aspect to note is a general clustering by color, that is the TOA radiation errors are qualitatively different for different times and dates due to different cloud characteristics across the cases. However, within each case there are generally consistent responses to the sensitivity experiments. The reduced INP simulations (SOC and V21 compared to control) broadly result in lower LW fluxes by up to 10 W m⁻² and higher SW fluxes by 5–50 W m⁻² (except for the 19 February 2023 15:00 UTC pass, gray symbols). The magnitude differs across cases. For example, the impact is small on 6 February 2023 15:00 UTC when the cloud mostly consists of supercooled liquid water (Figure 6) whereas there is greater sensitivity on 6 February 2023 18:00 UTC when the clouds are mixed-phase (Figure 7). The difference between the V21 and SOC simulations only has a noteworthy impact on the 19 February 2023.

Reducing INP toward the observed does not consistently result in improved TOA fluxes compared to observed; it improves the SW errors when they are negative but exacerbates the positive SW errors. Reducing Nd toward the observed results in dimmer clouds with a consistent reduction in TOA SW flux by 20–40 W m⁻² and a relatively small reduction in TOA LW flux. However, similar to the impact of the INP, the reduction in Nd does not consistently result in improved simulations of TOA fluxes; for example, at 18:00 UTC 7 February 2023 the error reduces from 25 to -6 W m⁻² but at 15:00 UTC 6 February 2023 the SW error increases from -15 W m⁻² in the SOC simulations to -50 W m⁻².

Changing MPOF has a similar impact as changing INP with MPOF1 decreasing the TOA SW flux by $20-50\,\mathrm{W}\,\mathrm{m}^{-2}$. In cases with high sensitivity to INP there is also higher sensitivity to MPOF as both have more impact on mixed phase cloud and less impact on supercooled liquid clouds or ice dominant clouds. These clouds must also be more broken to see the impact of MPOF. Again, neither MPOF simulation results in consistently improved TOA fluxes.

The different errors seen across the cases are a result of various case-by-case simulation deficiencies. For example, on the 6 February 2023 at 18:00 UTC and 21:00 UTC, and 7 February 2023 at 15:00 UTC there are relatively large errors in both short and long wave radiation which are caused by too much cloud above the flight in the model. Flight 385 leg 2 is the closest flight leg to 21:00 UTC on the 6 February 2023, the additional snow falling into the lower-level cloud is caused by frontal cloud being too thick. The frontal cloud is also the cause of

SMITH ET AL. 15 of 22

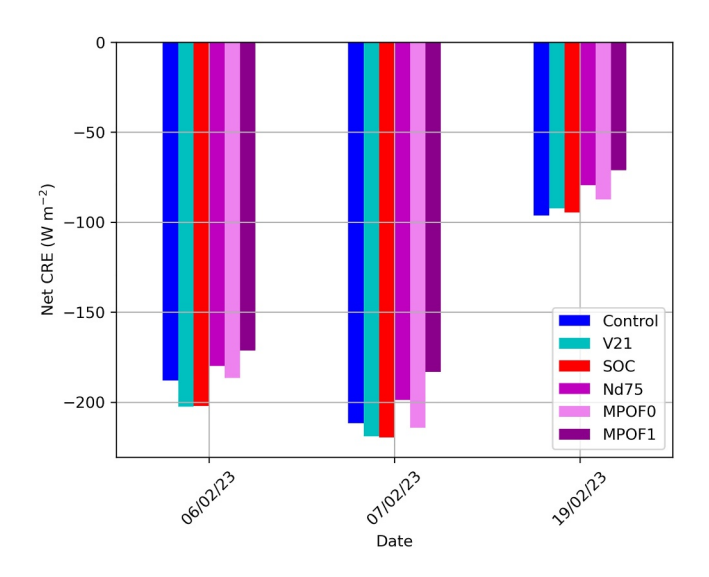


Figure 12. Mean surface net cloud radiative effect, CRE (W m $^{-2}$), from 12 UTC to 00 UTC for all three case studies and for the six sensitivity tests averaged over the area in the blue box in Figure 1.

the radiation errors. Some additional unexpected cloud was also present during flight 386 coincident with 15:00 UTC 7 February 2023. At 15:00 UTC 6 February 2023, coincident with flight 384, the cloud was too broken and LWC too low explaining the SW errors, however the LW error is difficult to explain from the aircraft data as the cloud top height was well simulated and broken cloud would lead to a positive error. At 18:00 UTC and 21:00 UTC 7 February 2023 and 21:00 UTC 9 February 2023 have comparatively modest errors. The droplet numbers during flight 387 are close to the campaign average, hence the improved TOA SW at 18:00 UTC 7 February 2023 in the simulation with the reduced droplet number. At 21:00 UTC 7 February 2023 the model appears to have cloud that is not optically thick enough. At 21:00 UTC 19 February 2023 there was only a small amount of patchy cloud simulated and observed, hence the small errors and sensitivities.

In summary, the MetUM TOA fluxes are sensitive to the choice of INP, Nd, and MPOF by similar magnitude and generally in the same way across all 8 comparisons - but dependent on the cloud characteristics. Constraining these toward the observed cloud properties does not consistently improve the TOA fluxes. Unfortunately, improvement is case dependent.

4.4. Surface Cloud Radiative Effect

It is pertinent to assess the impacts of the cloud representation on the surface radiation flux. The surface cloud radiative effect (CRE) is defined as the

amount of radiation reaching the surface minus the amount that would reach the surface if there were not any clouds. A positive value would be an increase in the amount of radiation reaching the surface and a negative value would be a decrease caused by the presence of clouds. Figure 12 shows the 12-hr average net cloud radiative effect between 12 UTC and 00 UTC for all three cases. All cases have a negative CRE, the clouds reduce the amount of radiation reaching the surface, with this dominantly a SW effect (not shown). The value is smaller on the 19 February 2023 as there was less cloud. The changes in CRE from the sensitivity experiments are typically ± 20 –30 W m⁻² averaged over our 43,000 km² box, so substantial.

Comparing the SOC simulation with the control (Figure 13a) shows that reducing the INP causes the CRE to become more negative by up to 14 W m⁻² (Figure 12). Although, not quantified in the same manner, the impact of reducing INP has a similar impact (more negative) to the simulations reducing INP in Vignon et al. (2021). The difference between the SOC simulation and V21 is small, suggesting that the variability in INP around coastal Antarctica has a limited impact on the CRE when at these low concentrations. The reduction in Nd results in an increase in CRE by 22 W m⁻² (Figure 13b) as a result of clouds with lower albedo and changes to the cloud amount. Comparing the reduced Nd with the control demonstrates that the biases in the droplet number and INP can partially compensate, but that the reduction in droplet number has a larger impact on CRE (Figure 13c). Similarly, MPOF has a significant impact on the CRE. The MPOF0 run has a higher CRE than the MPOF1 by up to 31 W m⁻² as a result of the increased liquid phase and decreased ice phase discussed in Section 4.1 and 4.2. Finney et al. (2025) explored the sensitivity of TOA SW CRE for convective anvil clouds to Nd, MPOF and INP demonstrating similar impacts. However, they found a relatively small impact from INP and MPOF and much larger impact from Nd. The difference in the sensitivities is influenced by the difference in cloud morphology, for example, our cases with lower cloud fractions are likely lower cloud fractions than Finney et al. (2025) and therefore more sensitive to MPOF.

In summary, all three processes can have a similar impact on the cloud radiative effect further highlighting the need to constrain all three processes in models over the Southern Ocean.

5. Discussion

Using the operational configuration of CASIM in the MetUM (Field et al., 2023), we have shown that the model is sensitive to the choice of droplet number concentration and the temperature dependent INP scheme. Observations of Nd over the SO and coastal Antarctica on average range from 28 to 155 cm⁻³ (e.g., Huang et al., 2017; Lachlan-Cope et al., 2016). Additionally, we have shown that representing the observed smaller INP concentrations is

SMITH ET AL. 16 of 22



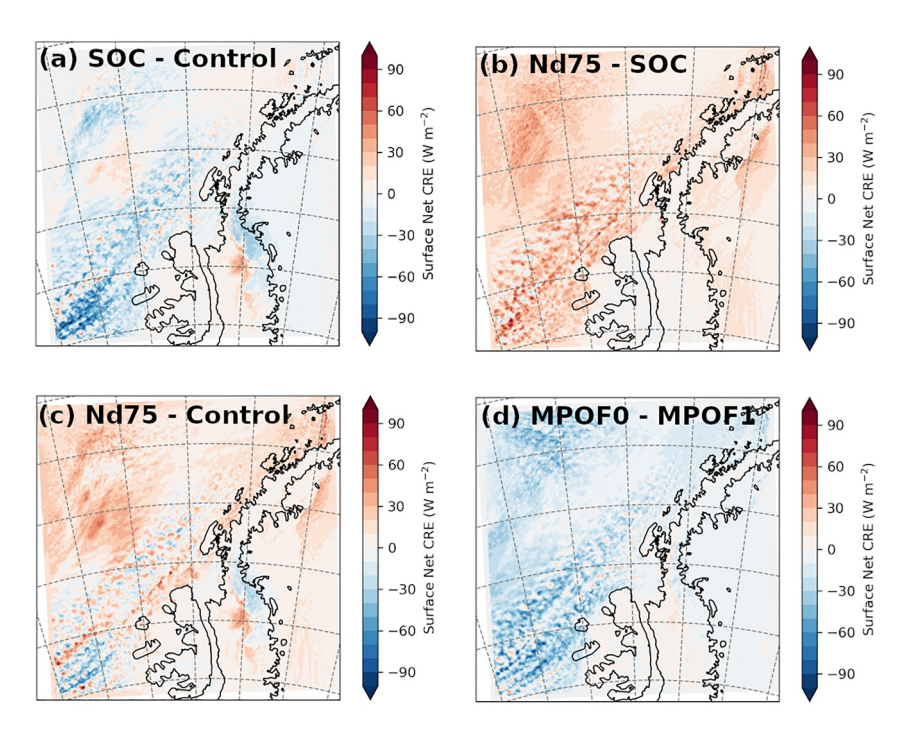


Figure 13. Mean surface net cloud radiative effect (W m⁻²) difference between the SOC and control (a), the Nd75 and SOC (b), the Nd 75 and control (c), and the MPOF 0 and MPOF 1 experiments (d) from 12 UTC 6 February 2023 to 00 UTC 7 February 2023.

important to accurately simulate clouds, but these clouds have little sensitivity to difference between two different coastal Antarctic INP schemes (SOC and V21). CASIM can be configured with activation schemes for cloud droplet activation (e.g., Abdul-Razzak & Ghan, 2000) and with aerosol dependent INP schemes (Miltenberger et al., 2020). These aerosol aware schemes will also need to be assessed for simulating clouds over the SO and for any benefit, in terms of the CRE, they offer over the current operational approach. Other modeling studies have shown that increased complexity does result in more accurate simulations of cloud fraction, liquid hydrometers, and CRE (Hines et al., 2019). Similarly, improvements in supercooled liquid clouds in CAM6 compared to CAM5 were largely due to changing from a temperature dependent INP scheme to an aerosol aware scheme (Gettelman et al., 2020). Recently, a set of aerosol aware INP schemes were evaluated offline forced by a global model with a detailed aerosol component (Herbert et al., 2025) and an optimized scheme was produced. Simulating clouds over SO using this scheme within CASIM should be evaluated.

The negative cloud-phase feedback, which in a warming world will result in a state with more liquid water and a greater albedo which results in a cooling, is an important component of the climate system (Bjordal et al., 2020). Furthermore, the concentration of INPs plays a crucial role in the magnitude of this feedback (Murray et al., 2021). While other studies have discussed the role of accurately representing droplet number concentrations and INPs, here we have also demonstrated that the amount of phase mixing in a model grid cell (via MPOF) impacts the TOA radiation balance and surface CRE in mixed-phase clouds to a similar degree, therefore, how well-mixed mixed-phase cloud are represented will also affect the strength of the negative cloud-phase feedback in models.

We have shown the importance of MPOF, the parameter that controls the distribution in phase of water in clouds, and the sensitivity to the fixed value assigned to this parameter. Recent work has derived an optimal value for MPOF (0.7–0.85) based on aircraft observations from the northern hemisphere (Evans et al., 2025). Performing a similar examination over the Southern Ocean, to understand hemispheric differences, would be important to help improve simulations over the Southern Ocean. One potential improvement would be for MPOF to be a physically based function of, for example, temperature or sub-grid turbulence as suggested by Korolev (2008) and Korolev and Milbrandt (2022). The optimal value of MPOF is between the value used in our MPOF1 and Nd75 simulations which suggests these two simulations are those configured most closely to observations. In addition, it

SMITH ET AL. 17 of 22

Online Library on [27/11/2025]. See

should be noted that MPOF is closely linked to accurately simulating the ice and liquid cloud fractions from the macroscale cloud scheme. The macroscale cloud scheme can have an important impact on cloud phase and the radiation budget in the simulations of low-level mixed-phase clouds (Van Weverberg et al., 2023).

We have examined clouds within the temperature range of the Hallet-Mossop rime splintering process. Secondary ice production processes can affect mixed-phased clouds but these processes remain poorly constrained or unrepresented in models (Atlas et al., 2022; Hoose, 2022; Sotiropoulou et al., 2021; Young et al., 2019). A detailed assessment of our observations during the SOC special observing periods focusing on secondary ice production will be part of future research. Future work should also examine the Hallet-Mossop process within the MetUM as well as the impact of only representing one secondary ice process.

The TOA radiation errors were often larger than the sensitivity to the mixed-phase cloud processes suggesting other processes were responsible for the errors. One deficiency noted in the simulated meteorological structure was in the cloud top temperature inversion strength. Previous studies have demonstrated that higher vertical resolution can improve the representation of mixed-phase clouds (Barrett et al., 2017), however, this comes at additional computational cost. Alternatively, the parametrization of cloud top turbulence and turbulence more broadly should be examined in terms of representing clouds over the SO (Price et al., 2025; Vignon et al., 2021). Although we didn't find any systematic temperature and humidity errors, a previous study comparing the MetUM with CASIM against satellite and shipborne remote sensing measurements over the Australian sector of the SO and found that the modeled cloud was sensitive to the driving model, ice processes, droplet number concentration and boundary layer mixing with meteorological errors inherited from the driving model are a leading cause of poorly simulated clouds (Price et al., 2025).

6. Conclusions

We have evaluated the performance of the MetUM in simulating clouds over the Southern Ocean using aircraft and satellite data during the Southern Ocean Clouds SOP1 field campaign in February 2023. In low-level cloud, the control MetUM produced too much ice when comparing in-cloud microphysical parameters with aircraft observations, a common issue in modeled clouds over the Southern Ocean, which results in errors in radiative fluxes.

A set of sensitivity tests were performed to understand the sensitivity of modeled cloud, and their radiative effect to uncertainties in mixed-phase clouds processes. Namely, ice nucleating particle number concentration, cloud droplet number concentration and how well mixed the different phases are within a grid-box—a parameter known as the mixed phase overlap factor controls this within the MetUM.

Reducing the INP, from the MetUM default (Cooper, 1987), to the observed concentrations from the Southern Ocean Clouds special observing period results in a reduction of ice and snow in the model, albeit to amounts still greater than observed (ice was modeled when it wasn't observed). The reduced ice and snow have a considerable impact on the radiation in the study region, highlighting the importance of correctly simulating the magnitude of the INP. A comparison between the SOC parametrization and an alternative parametrization for a different Antarctic coastal region (Vignon et al., 2021) showed little sensitivity in cloud microphysics, radiation balance and consequently cloud radiative effect. This lack of sensitivity demonstrates that representing the order of magnitude of INP over the Southern Ocean is critical. However, for models using temperature dependent INP schemes, once the right order of magnitude is presented, variations around that have little impact. Future studies should examine more complex aerosol aware INP schemes with scavenging and recycling of INP to better understand the impact of INP variability.

Reducing the Nd to the campaign average was also critical. It had a similar sized impact on cloud radiative effect (up to 22 W m⁻²), to INP changes (up to 14 W m⁻²), but opposite in sign. This highlights that errors in the cloud droplet number concentration and INP can partially compensate, producing TOA fluxes closer to observed but for the wrong reason. Changing these two parameters results in TOA radiation impacts that are a difference between the two effects. The compensation makes it hard to achieve more accurate results across multiple case studies (Figure 11).

We have also shown that the model is sensitive to the mixed-phase overlap factor or in other words whether the mixed-phased clouds are represented as conditionally or genuinely mixed. The sensitivity of the cloud radiative

SMITH ET AL. 18 of 22

21698996, 2025, 23, Downlo

elibrary.wiley.com/doi/10.1029/2025JD044452 by British

effect to MPOF demonstrates that accurately modeling how well mixed mixed-phase clouds are over the Southern Ocean is critical for modeling the radiation balance.

Our study focusses on three key components of the CASIM microphysics scheme in its current operational configuration. We acknowledge that other processes play a key role, and increased complexity could offer benefit. However, we have shown that the parametrization of INP, cloud droplet number concentration and the liquid and ice phase overlap all play a crucial role in correctly modeling mixed-phase clouds and their impact on the radiation budget over the Southern Ocean.

Conflict of Interest

The authors declare no conflicts of interest relevant to this study.

Data Availability Statement

The Southern Ocean Clouds aircraft observations will be made available on https://data.ceda.ac.uk/badc. The ice nucleation particle measurements are available at van den Heuvel et al. (2025). The CERES SSF is available from https://ceres.larc.nasa.gov/data/. The ACESPACE ice nucleating particle observations are available at Tatzelt et al. (2020). Owing to intellectual property rights restrictions, we cannot provide the source code or documentation papers for the UM. The MetUM is available for use under license. A number of research organizations and national meteorological services use the UM in collaboration with the Met Office to undertake basic atmospheric process research, produce forecasts, and develop the UM code. To apply for a license, see http://www.metoffice.gov.uk/research/modelling-systems/unified-model. CASIM is open source (BSD3 license) and it is available from https://code.metoffice.gov.uk, which requires registration. MetUM was run using Rose Suite Number u-cz325. The processed MetUM output is available at Smith (2025).

Acknowledgments

The Southern Ocean Clouds project was supported by the Natural Environment Research Council (NERC) as part of the CloudSense Programme and it was funded by the project Grant NE/T006404/1. The authors would like to thank everyone based at Rothera Research station who have supported the collection of observations. We would like to thank Jonathan Witherstone, the MASIN engineer, for support with the aircraft operations. We also thank the members of the CloudSense Programme for useful discussions and feedback on the work. We acknowledge use of the Monsoon2 system, a collaborative facility supplied under the Joint Weather and Climate Research Programme, a strategic partnership between the Met Office and the Natural Environment Research Council. We would like to thank the three anonymous reviewers for their constructive feedback, which improved the final manuscript.

References

- Abdul-Razzak, H., & Ghan, S. (2000). A parameterization of aerosol activation 2. Multiple aerosol types. *Journal of Geophysical Research*, 105(D5), 6837–6844. https://doi.org/10.1029/1999JD901161
- Abel, S. J., Boutle, I. A., Waite, K., Fox, S., Brown, P. R., Cotton, R., et al. (2017). The role of precipitation in controlling the transition from stratocumulus to cumulus clouds in a Northern Hemisphere cold-air outbreak. *Journal of the Atmospheric Sciences*, 74(7), 2293–2314. https://doi.org/10.1175/jas-d-16-0362.1
- Atlas, R. L., Bretherton, C. S., Blossey, P. N., Gettelman, A., Bardeen, C., Lin, P., & Ming, Y. (2020). How well do large-eddy simulations and global climate models represent observed boundary layer structures and low clouds over the summertime Southern Ocean? *Journal of Advances in Modeling Earth Systems*, 12(11), e2020MS002205. https://doi.org/10.1029/2020ms002205
- Atlas, R. L., Bretherton, C. S., Khairoutdinov, M. F., & Blossey, P. N. (2022). Hallett-Mossop rime splintering dims cumulus clouds over the Southern Ocean: New insight from nudged global storm-resolving simulations. *AGU Advances*, 3(2), e2021AV000454. https://doi.org/10.1030/000454
- Barrett, A. I., Hogan, R. J., & Forbes, R. M. (2017). Why are mixed-phase altocumulus clouds poorly predicted by large-scale models? Part 2. Vertical resolution sensitivity and parameterization. *Journal of Geophysical Research: Atmospheres*, 122(18), 9927–9944. https://doi.org/10.1002/2016[D026322]
- Baumgardner, D., Jonsson, H., Dawson, W., O'Connor, D., & Newton, R. (2001). The cloud, aerosol and precipitation spectrometer: A new instrument for cloud investigations. Atmospheric Research, 59–60, 251–264. https://doi.org/10.1016/S0169-8095(01)00119-3
- Baumgardner, D., Newton, R., Krämer, M., Meyer, J., Beyer, A., Wendisch, M., & Vochezer, P. (2014). The cloud particle spectrometer with polarization detection (CPSPD): A next generation open-path cloud probe for distinguishing liquid cloud droplets from ice crystals. *Atmospheric Research*, 142, 2–14. https://doi.org/10.1016/j.atmosres.2013.12.010
- Bergeron, T. (1935). On the physics of clouds and precipitation. In *Proces Verbaux de l'Association de Météorologie*. International Union of Geodesy and Geophysics.
- Best, M. J., Pryor, M., Clark, D. B., Rooney, G., Essery, R. L. H., Menard, C. B., et al. (2011). The joint UK land environment simulator (JULES), model description Part 1: Energy and water fluxes. *Geoscientific Model Development*, 4(3), 677–699. https://doi.org/10.5194/gmd-4-677-
- Bigg, E. K. (1953). The supercooling of water. Proceedings of the Physical Society Section B, 66(8), 688–694. https://doi.org/10.1088/0370-1301/66/8/309
- Bjordal, J., Storelvmo, T., Alterskjær, K., & Carlsen, T. (2020). Equilibrium climate sensitivity above 5°C plausible due to state-dependent cloud feedback. *Nature Geoscience*, 13(11), 718–721. https://doi.org/10.1038/s41561-020-00649-1
- Bodas-Salcedo, A., Mulcahy, J. P., Andrews, T., Williams, K. D., Ringer, M. A., Field, P. R., & Elsaesser, G. S. (2019). Strong dependence of atmospheric feedbacks on mixed-phase microphysics and aerosol-cloud interactions in HadGEM3. *Journal of Advances in Modeling Earth Systems*, 11(6), 1735–1758. https://doi.org/10.1029/2019ms001688
- Bodas-Salcedo, A., Williams, K. D., Ringer, M. A., Beau, I., Cole, J. N. S., Dufresne, J.-L., et al. (2014). Origins of the solar radiation biases over the Southern Ocean in CFMIP2 models. *Journal of Climate*, 27(1), 41–56. https://doi.org/10.1175/jcli-d-13-00169.1
- Bush, M., Boutle, I., Edwards, J., Finnenkoetter, A., Franklin, C., Hanley, K., et al. (2023). The second Met Office Unified Model–JULES regional atmosphere and land configuration. RAL2, Geosci. Model Dev., 16(6), 1713–1734. https://doi.org/10.5194/gmd-16-1713-2023

SMITH ET AL. 19 of 22

21698996

- Bush, M., Flack, D. L. A., Lewis, H. W., Bohnenstengel, S. I., Short, C. J., Franklin, C., et al. (2025). The third Met Office Unified Model–JULES regional atmosphere and land configuration, RAL3. Geoscientific Model Development Discussions, 18, 3819–3855. https://doi.org/10.5194/gmd-18-3819-2025
- Cesana, G., Khadir, T., Chepfer, H., & Chiriaco, M. (2022). Southern Ocean solar reflection biases in CMIP6 models linked to cloud phase and vertical structure representations. *Geophysical Research Letters*, 49(22), e2022GL099777. https://doi.org/10.1029/2022GL099777
- Cooper, W. A. (1987). Ice initiation in natural clouds. In *Precipitation enhancement—A scientific challenge*. In *Meteorological monographs* (Vol. 43, pp. 29–32). Springer. https://doi.org/10.1007/978-1-935704-17-1 4
- Cotton, R. J., Field, P. R., Ulanowski, Z., Kaye, P. H., Hirst, E., Greenaway, R. S., et al. (2013). The effective density of small ice particles obtained from *in situ* aircraft observations of mid-latitude cirrus. *Quarterly Journal of the Royal Meteorological Society*, 139(676), 1923–1934. https://doi.org/10.1002/qj.2058
- Crosier, J., Bower, K. N., Choularton, T. W., Westbrook, C. D., Connolly, P. J., Cui, Z. Q., et al. (2011). Observations of ice multiplication in a weakly convective cell embedded in supercooled mid-level stratus. *Atmospheric Chemistry and Physics*, 11(1), 257–273. https://doi.org/10.5194/acp-11-257-2011
- D'Alessandro, J. J., McFarquhar, G. M., Wu, W., Stith, J. L., Jensen, J. B., & Rauber, R. M. (2021). Characterizing the occurrence and spatial heterogeneity of liquid, ice and mixed phase low-level clouds over the Southern Ocean using in situ observations acquired during SOCRATES. *Journal of Geophysical Research: Atmospheres*, 126(11), e2020JD034482. https://doi.org/10.1029/2020JD034482
- DeMott, P. J., Prenni, A. J., Liu, X., Kreidenweis, S. M., Petters, M. D., Twohy, C. H., et al. (2010). Predicting global atmospheric ice nuclei distributions and their impacts on climate. *Proceedings of the National Academy of Sciences of the United States of America*, 107(25), 11217–11222. https://doi.org/10.1073/pnas.0910818107
- Elvidge, A. D., Renfrew, I. A., King, J. C., Orr, A., Lachlan-Cope, T. A., Weeks, M., & Gray, S. L. (2015). Foehn jets over the Larsen C Ice Shelf, Antarctica. *Quarterly Journal of the Royal Meteorological Society*, 141(688), 698–713. https://doi.org/10.1002/gi.2382
- Evans, M. D., Abel, S. J., Field, P. R., Finney, D. L., Lloyd, G., Cotton, R. J., et al. (2025). Characterising the spatial overlap between liquid and ice in mixed-phase clouds. *Quarterly Journal of the Royal Meteorological Society*, e5041. https://doi.org/10.1002/qj.5041
- Fiddes, S. L., Protat, A., Mallet, M. D., Alexander, S. P., & Woodhouse, M. T. (2022). Southern Ocean cloud and shortwave radiation biases in a nudged climate model simulation: Does the model ever get it right? *Atmospheric Chemistry and Physics*, 22, 14603–14630. https://doi.org/10.5194/acp-22-14603-2022
- Fiedler, E., Lachlan-Cope, T., Renfrew, I. A., & King, J. C. (2010). Convective heat transfer of thin-ice covered polynyas. *Journal of Geophysical Research*, 115, C10051. https://doi.org/10.1029/2009JC005797
- Field, P. R., Hill, A., Shipway, B., Furtado, K., Wilkinson, J., Miltenberger, A., et al. (2023). Implementation of a double moment cloud microphysics scheme in the UK met office regional numerical weather prediction model. *Quarterly Journal of the Royal Meteorological Society*, 149(752), 703–739. https://doi.org/10.1002/qj.4414
- Field, P. R., Hogan, R. J., Brown, P. R. A., Illingworth, A. J., Choularton, T. W., Kaye, P. H., et al. (2004). Simultaneous radar and aircraft observations of mixed-phase cloud at the 100 m scale. *Quarterly Journal of the Royal Meteorological Society*, 130(600), 1877–1904. https://doi.org/10.1256/qj.03.102
- Findeisen, W. (1938). Die kolloidmeteorologischen Vorgänge bei der Niederschlagsbildung. Meteorologische Zeitschrift, 55, 121–133. https://doi.org/10.1127/metz/2015/0675
- Finney, D. L., Blyth, A. M., Field, P. R., Daily, M. I., Murray, B. J., Sun, M., et al. (2025). Microphysical fingerprints in anvil cloud albedo. EGUsphere, 25(18), 10907–10929. https://doi.org/10.5194/acp-25-10907-2025
- Gettelman, A., Bardeen, C. G., McCluskey, C. S., Järvinen, E., Stith, J., Bretherton, C., et al. (2020). Simulating observations of Southern Ocean clouds and implications for climate. *Journal of Geophysical Research: Atmospheres*, 125(21), e2020JD032619. https://doi.org/10.1029/2020JD032619
- Gilbert, E., Orr, A., King, J. C., Renfrew, I. A., Lachlan-Cope, T., Field, P. R., & Boutle, I. A. (2020). Summertime cloud phase strongly influences surface melting on the Larsen C ice shelf, Antarctica. *Quarterly Journal of the Royal Meteorological Society*, 146(729), 1575–1589. https://doi.org/10.1002/qj.3753
- Grosvenor, D. P., Field, P. R., Hill, A. A., & Shipway, B. J. (2017). The relative importance of macrophysical and cloud albedo changes for aerosol-induced radiative effects in closed-cell stratocumulus: Insight from the modelling of a case study. *Atmospheric Chemistry and Physics*, 17(8), 5155–5183. https://doi.org/10.5194/acp-17-5155-2017
- Hallett, J., & Mossop, S. C. (1974). Production of secondary ice particles during the riming process. Nature, 249(5452), 26–28. https://doi.org/10.1038/249026a0
- Hansen, N., Orr, A., Zou, X., Boberg, F., Bracegirdle, T. J., Gilbert, E., et al. (2024). The importance of cloud properties when assessing surface melting in an offline-coupled firn model over Ross Ice shelf, West Antarctica. The Cryosphere, 18(6), 2897–2916. https://doi.org/10.5194/tc-18-2897-2024
- Hawker, R. E., Miltenberger, A. K., Johnson, J. S., Wilkinson, J. M., Hill, A. A., Shipway, B. J., et al. (2021). Model emulation to understand the joint effects of ice-nucleating particles and secondary ice production on deep convective anvil cirrus. *Atmospheric Chemistry and Physics*, 21(23), 17315–17343. https://doi.org/10.5194/acp-21-17315-2021
- Herbert, R. J., Sanchez-Marroquin, A., Grosvenor, D. P., Pringle, K. J., Arnold, S. R., Murray, B. J., & Carslaw, K. S. (2025). Gaps in our understanding of ice-nucleating particle sources exposed by global simulation of the UK Earth System Model. Atmospheric Chemistry and Physics, 25(1), 291–325. https://doi.org/10.5194/acp-25-291-2025
- Hill, A. A., Shipway, B. J., & Boutle, I. A. (2015). How sensitive are aerosol-precipitation interactions to the warm rain representation? *Journal of Advances in Modeling Earth Systems*, 7(3), 987–1004. https://doi.org/10.1002/2014MS000422
- Hines, K. M., Bromwich, D. H., Wang, S.-H., Silber, I., Verlinde, J., & Lubin, D. (2019). Microphysics of summer clouds in central West Antarctica simulated by the Polar Weather Research and Forecasting Model (WRF) and the Antarctic Mesoscale Prediction System (AMPS). Atmospheric Chemistry and Physics, 19, 12431–12454. https://doi.org/10.5194/acp-19-12431-2019
- Hoose, C. (2022). Another piece of evidence for important but uncertain ice multiplication processes. AGU Advances, 3(2), e2022AV000669. https://doi.org/10.1029/2022AV000669
- Huang, X., Field, P. R., Murray, B. J., Grosvenor, D. P., van den Heuvel, F., & Carslaw, K. S. (2025). Different responses of cold-air outbreak clouds to aerosol and ice production depending on cloud temperature. Atmospheric Chemistry and Physics, 25, 11363–11406. https://doi.org/ 10.5194/acp-25-11363-2025
- Huang, Y., Chubb, T., Baumgardner, D., deHoog, M., Siems, S. T., & Manton, M. J. (2017). Evidence for secondary ice production in Southern Ocean open cellular convection. *Quarterly Journal of the Royal Meteorological Society*, 143(704), 1685–1703. https://doi.org/10.1002/qj.3041
 Hyder, P., Edwards, J. M., Allan, R. P., Hewitt, H. T., Bracegirdle, T. J., Gregory, J. M., et al. (2018). Critical Southern Ocean climate model biases traced to atmospheric model cloud errors. *Nature Communications*, 9(1), 1–17. https://doi.org/10.1038/s41467-018-05634-2

SMITH ET AL. 20 of 22

21698996



Journal of Geophysical Research: Atmospheres

- 10.1029/2025JD044452
- Järvinen, E., McCluskey, C. S., Waitz, F., Schnaiter, M., Bansemer, A., Bardeen, C. G., et al. (2022). Evidence for secondary ice production in southern ocean maritime boundary layer clouds. *Journal of Geophysical Research: Atmospheres*, 127(16), e2021JD036411. https://doi.org/10.1029/2021JD036411
- Khairoutdinov, M., & Kogan, Y. (2000). A new cloud physics parameterization in a large-eddy simulation model of marine stratocumulus. Monthly Weather Review, 128(1), 229–243. https://doi.org/10.1175/1520-0493(2000)128<0229;ANCPPI>2.0.CO;2
- King, J. C., Lachlan-Cope, T. A., Ladkin, R. S., & Weiss, A. (2008). Airborne measurements in the stable boundary layer over the Larsen Ice Shelf, Antarctica. Boundary-Layer Meteorology, 127(3), 413–428. https://doi.org/10.1007/s10546-008-9271-4
- Korolev, A., & Milbrandt, J. (2022). How are mixed-phase clouds mixed? Geophysical Research Letters, 49(18), e2022GL099578. https://doi.org/10.1029/2022GL099578
- Korolev, A. V. (2008). Rates of phase transformations in mixed-phase clouds. Quarterly Journal of the Royal Meteorological Society, 134(632), 595–608. https://doi.org/10.1002/qj.230
- Korolev, A. V., Emery, E. F., Strapp, J. W., Cober, S. G., Isaac, G. A., Wasey, M., & Marcotte, D. (2011). Small ice particles in tropospheric clouds: Fact or artifact? Airborne icing instrumentation evaluation experiment. *Bulletin of the American Meteorological Society*, 92(8), 967–973. https://doi.org/10.1175/2010BAMS3141.1
- Lachlan-Cope, T., & the Southern Ocean Clouds team. (2025). Have three years of observations explained model biases in Southern Ocean clouds? In EGU General Assembly 2025, Vienna, Austria, 27 Apr-2 May 2025, EGU25-12746. https://doi.org/10.5194/egusphere-egu25-12746
- Lachlan-Cope, T., Listowski, C., & O'Shea, S. (2016). The microphysics of clouds over the Antarctic Peninsula–Part 1: Observations. Atmospheric Chemistry and Physics. 16(24), 15605–15617. https://doi.org/10.5194/acp-16-15605-2016
- Lance, S., Brock, C. A., Rogers, D., & Gordon, J. A. (2010). Water droplet calibration of the Cloud Droplet Probe (CDP) and in-flight performance in liquid, ice and mixed-phase clouds during ARCPAC. Atmospheric Measurement Techniques, 3(6), 1683–1706. https://doi.org/10.5194/amt-3-1683-2010
- Lauer, A., Bock, L., Hassler, B., Schröder, M., & Stengel, M. (2022). Cloud climatologies from global climate models—A comparison of CMIP5 and CMIP6 models with satellite data. *Journal of Climate*, 36(2), 281–311. https://doi.org/10.1175/JCLI-D-22-0181.1
- Lauer, A., Jones, C., Eyring, V., Evaldsson, M., Hagemann, S., Mäkelä, J., et al. (2018). Process-level improvements in CMIP5 models and their impact on tropical variability, the Southern Ocean, and monsoons. *Earth System Dynamics*, 9(1), 33–67. https://doi.org/10.5194/esd-9-33-2018
- Lawson, R. P., O'Connor, D., Zmarzly, P., Weaver, K., Baker, B., Mo, Q., & Jonsson, H. (2006). The 2D-S (stereo) probe: Design and preliminary tests of a new airborne, high-speed, high-resolution particle imaging probe. *Journal Atmosphere Ocean Technology*, 23, 1462–1477. https://doi.org/10.1175/JTECH1927.1
- Listowski, C., & Lachlan-Cope, T. (2017). The microphysics of clouds over the Antarctic Peninsula—Part 2: Modelling aspects within Polar WRF. Atmospheric Chemistry and Physics, 17(17), 10195–10221. https://doi.org/10.5194/acp-17-10195-2017
- Loeb, N. G., Manalo-Smith, N., Su, W., Shankar, M., & Thomas, S. (2016). CERES top-of-atmosphere Earth radiation budget climate data record: Accounting for in-orbit changes in instrument calibration. Remote Sensing, 8(3), 182. https://doi.org/10.3390/rs8030182
- McCluskey, C. S., Hill, T. C. J., Humphries, R. S., Rauker, A. M., Moreau, S., Strutton, P. G., et al. (2018). Observations of ice nucleating particles over Southern Ocean waters. *Geophysical Research Letters*, 45(21), 989. https://doi.org/10.1029/2018GL079981
- McCoy, I. L., McCoy, D. T., Wood, R., Regayre, L., Watson-Parris, D., Grosvenor, D. P., et al. (2020). The hemispheric contrast in cloud microphysical properties constrains aerosol forcing. *Proceedings of the National Academy of Sciences of the United States of America*, 117(32), 18998–19006. https://doi.org/10.1073/pnas.1922502117
- McCusker, G. Y., Vüllers, J., Achtert, P., Field, P., Day, J. J., Forbes, R., et al. (2023). Evaluating Arctic clouds modelled with the Unified Model and Integrated Forecasting System. *Atmospheric Chemistry and Physics*, 23(8), 4819–4847. https://doi.org/10.5194/acp-23-4819-2023
- McFarquhar, G. M., Bretherton, C. S., Marchand, R., Protat, A., DeMott, P. J., Alexander, S. P., et al. (2021). Observations of clouds, aerosols, precipitation, and surface radiation over the Southern Ocean: An overview of CAPRICORN, MARCUS, MICRE, and SOCRATES. Bulletin of the American Meteorological Society, 102(4), E894–E928. https://doi.org/10.1175/bams-d-20-0132.1
- Miltenberger, A. K., Field, P. R., Hill, A. A., & Heymsfield, A. J. (2020). Vertical redistribution of moisture and aerosol in orographic mixed-phase clouds. *Atmospheric Chemistry and Physics*, 20(13), 7979–8001. https://doi.org/10.5194/acp-20-7979-2020
- Miltenberger, A. K., Field, P. R., Hill, A. A., Rosenberg, P., Shipway, B. J., Wilkinson, J. M., et al. (2018). Aerosol–cloud interactions in mixed-phase convective clouds–Part 1: Aerosol perturbations. *Atmospheric Chemistry and Physics*, 18(5), 3119–3145. https://doi.org/10.5194/acp-18-3119-2018
- Morrison, H., Curry, J. A., & Khvorostyanov, V. I. (2005). A new double-moment microphysics parameterization for application in cloud and climate models. Part I: Description, *Journal of the Atmospheric Sciences*, 62(6), 1665–1677. https://doi.org/10.1175/JAS3446.1
- Murray, B. J., Carslaw, K. S., & Field, P. R. (2021). Opinion: Cloud-phase climate feedback and the importance of ice-nucleating particles. Atmospheric Chemistry and Physics, 21(2), 665–679. https://doi.org/10.5194/acp-21-665-2021
- O'Shea, S. J., Choularton, T. W., Flynn, M., Bower, K. N., Gallagher, M., Crosier, J., et al. (2017). In situ measurements of cloud microphysics and aerosol over coastal Antarctica during the MAC campaign. *Atmospheric Chemistry and Physics*, 17(21), 13049–13070. https://doi.org/10.5194/acp-17-13049-2017
- Pei, Z., Fiddes, S. L., Mallet, M. D., Alexander, S. P., Furtado, K., Roff, G., et al. (2025). Simulating mixed-phase clouds over coastal Antarctica during a significant snowfall event in a high-resolution regional model. *Journal of Geophysical Research: Atmospheres*, 130(10), e2024JD042311. https://doi.org/10.1029/2024JD042311
- Pincus, R., & Baker, M. (1994). Effect of precipitation on the albedo susceptibility of clouds in the marine boundary layer. *Nature*, 372(6503), 250–252, https://doi.org/10.1038/372250a0
- Poku, C., Ross, A. N., Hill, A. A., Blyth, A. M., & Shipway, B. (2021). Is a more physical representation of aerosol activation needed for simulations of fog? Atmospheric Chemistry and Physics, 21(9), 7271–7292. https://doi.org/10.5194/acp-21-7271-2021
- Price, R., Orr, A., Field, P. F., Mace, G., & Protat, A. (2025). Simulation of cloud processes over offshore coastal Antarctica using the high-resolution regional UK Met Office Unified Model with interactive aerosols. *Journal of Geophysical Research: Atmospheres*, 130(4), e2024JD042109. https://doi.org/10.1029/2024JD042109
- Revell, L. E., Kremser, S., Hartery, S., Harvey, M., Mulcahy, J. P., Williams, J., et al. (2019). The sensitivity of Southern Ocean aerosols and cloud microphysics to sea spray and sulfate aerosol production in the HadGEM3-GA7. 1 Chemistry-climate model. Atmospheric Chemistry and Physics, 19(24), 15447–15466. https://doi.org/10.5194/acp-19-15447-2019
- Rosenberg, P. D., Dean, A. R., Williams, P. I., Dorsey, J. R., Minikin, A., Pickering, M. A., & Petzold, A. (2012). Particle sizing calibration with refractive index correction for light scattering optical particle counters and impacts upon PCASP and CDP data collected during the Fennec campaign. Atmospheric Measurement Techniques, 5, 1147–1163. https://doi.org/10.5194/amt-5-1147-2012

SMITH ET AL. 21 of 22

21698996



Journal of Geophysical Research: Atmospheres

- 10.1029/2025JD044452
- Sauerland, F., Souverijns, N., Possner, A., Wex, H., Van Overmeiren, P., Mangold, A., et al. (2024). Ice-nucleating particle concentration impacts cloud properties over Dronning Maud Land, East Antarctica, in COSMO-CLM². Atmospheric Chemistry and Physics, 24(23), 13751–13768. https://doi.org/10.5194/acp-24-13751-2024
- Shipway, B. J., & Hill, A. A. (2012). Diagnosis of systematic differences between multiple parametrizations of warm rain microphysics using a kinematic framework. *Quarterly Journal of the Royal Meteorological Society*, 138(669), 2196–2211. https://doi.org/10.1002/qj.1913
- Smith, D. (2025). MetUM data for "The impact of mixed-phase cloud processes on simulating Southern Ocean clouds and their radiative effect" manuscript [Dataset]. Zenodo. https://doi.org/10.5281/zenodo.15601588
- Sotiropoulou, G., Vignon, É., Young, G., Morrison, H., O'Shea, S. J., Lachlan-Cope, T., et al. (2021). Secondary ice production in summer clouds over the Antarctic coast: An underappreciated process in atmospheric models. *Atmospheric Chemistry and Physics*, 21(2), 755–771. https://doi.org/10.5194/acp-21-755-2021
- Stevens, B., Satoh, M., Auger, L., Biercamp, J., Bretherton, C. S., Chen, X., et al. (2019). Dyamond: The dynamics of the atmospheric general circulation modeled on non-hydrostatic domains. *Progress in Earth and Planetary Science*, 6(1), 61. https://doi.org/10.1186/s40645-019-0304-z
- Tan, I., & Storelvmo, T. (2016). Sensitivity study on the influence of cloud microphysical parameters on mixed-phase cloud thermodynamic phase partitioning in CAM5. *Journal of the Atmospheric Sciences*, 73(2), 709–728. https://doi.org/10.1175/JAS-D-15-0152.1
- Tatzelt, C., Henning, S., Tummon, F., Hartmann, M., Baccarini, A., Welti, A., et al. (2020). Ice nucleating particle number concentration from low-volume sampling over the Southern Ocean during the austral summer of 2016/2017 on board the Antarctic Circumnavigation Expedition (ACE) (version 1.1) [Dataset]. Zenodo. https://doi.org/10.5281/zenodo.4311665
- Uetake, J., Hill, T. C., Moore, K. A., DeMott, P. J., Protat, A., & Kreidenweis, S. M. (2020). Airborne bacteria confirm the pristine nature of the Southern Ocean boundary layer. *Proceedings of the National Academy of Sciences*, 117(24), 13275–13282. https://doi.org/10.1073/pnas.
- van den Heuvel, F., Lachlan-Cope, T., Kinney, N., & Smith, D. (2025). Ice Nucleating Particle concentrations from Rothera research station in Antarctica measured using the offline, wash-off filter method from filters which were exposed in February 2023 (version 1.0) [Dataset]. NERC EDS UK Polar Data Centre. https://doi.org/10.5285/AE7F3AEA-B0D4-401D-96E7-103EABB9DA34
- Van Weverberg, K., Giangrande, S., Zhang, D., Morcrette, C. J., & Field, P. R. (2023). On the role of macrophysics and microphysics in km-scale simulations of mixed-phase clouds during cold air outbreaks. *Journal of Geophysical Research: Atmospheres*, 128(11), e2022JD037854. https://doi.org/10.1029/2022JD037854
- Van Weverberg, K., Morcrette, C. J., Boutle, I., Furtado, K., & Field, P. R. (2021). A bimodal diagnostic cloud fraction parameterization. Part I: Motivating analysis and scheme description. *Monthly Weather Review*, 149(3), 841–857. https://doi.org/10.1175/MWR-D-20-0224.1
- Vergara-Temprado, J., Miltenberger, A. K., Furtado, K., Grosvenor, D. P., Shipway, B. J., Hill, A. A., et al. (2018). Strong control of Southern Ocean cloud reflectivity by ice-nucleating particles. *Proceedings of the National Academy of Sciences*, 115(11), 2687–2692. https://doi.org/10.1073/pnas.1721627115
- Vignon, É., Alexander, S. P., DeMott, P. J., Sotiropoulou, G., Gerber, F., Hill, T. C. J., et al. (2021). Challenging and improving the simulation of mid-level mixed-phase clouds over the high-latitude Southern Ocean. *Journal of Geophysical Research: Atmospheres*, 126(7), e2020JD033490. https://doi.org/10.1029/2020JD033490
- Wegener, A. (1911). Thermodynamik der atmosphäre.
- Wielicki, B. A., Barkstrom, B. R., Harrison, E. F., Lee III, R. B., Smith, G. L., & Cooper, J. E. (1996). Clouds and the Earth's Radiant Energy System (CERES): An Earth observing system experiment. *Bulletin of the American Meteorological Society*, 77(5), 853–868. https://doi.org/10.1175/1520-0477(1996)077<0853:CATERE>2.0.CO;2
- Wilson, D. R., & Ballard, S. P. (1999). A microphysically based precipitation scheme for the UK Meteorological Office Unified Model. *Quarterly Journal of the Royal Meteorological Society*, 125(557), 1607–1636. https://doi.org/10.1256/smsqj.55706
- Xue, J., Xiao, Z., Bromwich, D. H., & Bai, L. (2022). Polar WRF V4.1.1 simulation and evaluation for the Antarctic and Southern Ocean. Frontiers in Earth Science, 16(4), 1005–1024. https://doi.org/10.1007/s11707-022-0971-8
- Young, G., Lachlan-Cope, T., O'Shea, S. J., Dearden, C., Listowski, C., Bower, K. N., et al. (2019). Radiative effects of secondary ice enhancement in coastal Antarctic clouds. *Geophysical Research Letters*, 46(4), 2312–2321. https://doi.org/10.1029/2018GL080551
- Zhou, X., Atlas, R., McCoy, I. L., Bretherton, C. S., Bardeen, C., Gettelman, A., et al. (2021). Evaluation of cloud and precipitation simulations in CAM6 and AM4 using observations over the Southern Ocean. *Earth and Space Science*, 8(2), e2020EA001241. https://doi.org/10.1029/2020EA001241

References From the Supporting Information

- Budke, C., & Koop, T. (2015). BINARY: An optical freezing array for assessing temperature and time dependence of heterogeneous ice nucleation. Atmospheric Measurement Techniques, 8(2), 689–703. https://doi.org/10.5194/amt-8-689-2015
- Tobo, Y. (2016). An improved approach for measuring immersion freezing in large droplets over a wide temperature range. *Scientific Reports*, 6(1), 32930. https://doi.org/10.1038/srep32930
- Vali, G. (1971). Quantitative evaluation of experimental results an the heterogeneous freezing nucleation of supercooled liquids. *Journal of the Atmospheric Sciences*, 28(3), 402–409. https://doi.org/10.1175/1520-0469(1971)028<0402:OEOERA>2.0.CO;2
- Whale, T. F., Murray, B. J., O'Sullivan, D., Wilson, T. W., Umo, N. S., Baustian, K. J., et al. (2015). A technique for quantifying heterogeneous ice nucleation in microlitre supercooled water droplets. *Atmospheric Measurement Techniques*, 8, 2437–2447. https://doi.org/10.5194/amt-8-2437-2015

SMITH ET AL. 22 of 22